Adipocyte PI3K Links Adipostasis with Basal Insulin Secretion Through an Adipoincretin Effect

Barbara Becattini[1], Angela Molinaro[1,2], Marcus Henricsson[1], Jan Borén[1], and Giovanni Solinas[1*]

1 Department of Molecular and Clinical Medicine, Institute of Medicine, University of Gothenburg, Gothenburg, Sweden.

2 Present address: Department of Laboratory Medicine, Institute of Medicine, University of Gothenburg, Gothenburg, Sweden.

[*]Correspondence: giovanni.solinas@wlab.gu.se

SUMMARY

Insulin secretion is governed by insulin-PI3K signaling. Resolving the mechanism of this feedback is necessary to understand how insulin operates. Mice lacking the insulin receptor, or AKT1 and AKT2 in adipocytes, are severely lipoatrophic. Thus, the role of adipocyte insulin-PI3K signaling in the control of insulin secretion remains unknown. Using adipocyte-specific PI3Kα knockout mice (PI3Kα^{AdQ}) and a panel of isoform-selective PI3K inhibitors, we have found that PI3Kα and PI3Kβ activities are functionally redundant in adipocyte insulin signaling. PI3Kβ-selective inhibitors had no effect on adipocyte AKT phosphorylation in control mice but blunted AKT phosphorylation specifically in adipocytes of PI3Kα^{AdQ} mice, demonstrating adipocyte-selective inhibition of PI3K signaling. Adipocyte-selective PI3K inhibition increased serum FFA and potently induced insulin secretion. We name this phenomenon the adipoincretin effect. The adipoincretin effect was dissociated from blood glucose and blood glucose counterregulatory response. The contribution of lipolysis, lipid, and amino acid metabolism, and selected adipokines to the adipoincretin effect has been investigated. We conclude that basal insulin secretion is chiefly controlled by adipocyte PI3K signaling through the adipoincretin effect. This phenomenon reveals an essential role for adipocyte insulin-PI3K signaling in linking the rates of adipose tissue lipolysis with baseline insulin secretion during fasting.

INTRODUCTION

Healthy humans with comparable blood glucose concentrations display a large variability in plasma insulin abundances (Kahn et al., 1993; Kodama et al., 2013), a phenomenon which is also observed between different strains of mice (Aston-Mourney et al., 2007). This capacity of different species to precisely match insulin secretion with insulin sensitivity over a wide range of serum insulin indicates a conserved crosstalk between the metabolic action of insulin and insulin secretion. The metabolic action of insulin depends on the induction of phosphoinositide-3 kinase (PI3K) - AKT signaling in insulin target cells (Solinas and Becattini, 2022). Pharmacological inhibition of either the insulin receptor (InsR), PI3K, or AKT causes hyperglycemia and hyperinsulinemia in humans and rodents (Ando et al., 2014; Hopkins et al., 2018; Kalinsky et al., 2018; Patnaik et al., 2016; von Mehren et al., 2020). Thus, insulin secretion is chiefly controlled by a conserved negative feedback mediated by InsR-PI3K signaling in a cell type yet to be identified. This feedback is assumed to be mediated by insulin action on blood glucose, which involves hepatic glucose production (Vasan and Cantley, 2022). Indeed, the current paradigm for the insulin system can be regarded as glucose-centric, with blood glucose being considered the primary driver of insulin secretion.

However, whereas PI3K inhibitors induce a large and sustained increase in insulin secretion in fasted C57BL/6 mice (Hopkins et al., 2018), a glucose injection in these mice causes only a modest and transient increase in plasma insulin (Aston-Mourney et al., 2007; Fergusson et al., 2014; Small et al., 2022). Moreover, hepatocyte-restricted acute inhibition of PI3K activity, achieved by administering a PI3Kβ-selective inhibitor to mice lacking PI3Kα in hepatocytes, causes hyperglycemia without further increasing insulin secretion (Molinaro et al., 2019). Altogether, this evidence made us question the current glucose-centric paradigm for the insulin system and motivated us to search for an alternative mechanism for the feedback linking insulin action with insulin secretion.

In humans and rodents, β-adrenergic agonists stimulate lipolysis and insulin secretion independently from blood glucose (Imura et al., 1971; Porte, 1967; Sennitt et al., 1985), and inhibition of lipolysis with nicotinic acid (NA) reduces insulin secretion during fasting (Balasse and Ooms, 1973; Boden et al., 1998; Dobbins et al., 1998a; Dobbins et al., 1998b; Stein et al., 1996). Furthermore, we have found that in humans with different adiposity and insulin sensitivity, fasting plasma insulin was not associated with blood glucose but was associated with adipose tissue lipolysis (Fryk et al., 2021). Considering the opposing actions of β-adrenergic signaling and InsR-PI3K signaling on adipocyte lipolysis (Guilherme et al., 2022; Solinas and Becattini, 2022), we hypothesized that insulin secretion is governed by adipocyte InsR-PI3K signaling.

68 Mice lacking either the InsR or AKT1 and AKT2 in their adipocytes develop severe
69 lipoatrophy and metabolic syndrome phenotype, demonstrating the requirement for
70 functional insulin signaling in adipostasis (Boucher et al., 2016; Qiang et al., 2016;
71 Sakaguchi et al., 2017; Shearin et al., 2016). However, because of their severely atrophic
72 adipose tissue and metabolic syndrome phenotype, these models provide limited insights
73 into the physiological role of InsR-PI3K signaling within the mature adipocyte. Thus, the role
74 of adipocyte PI3K signaling in the feedback controlling insulin secretion remains unknown.
75
76 **RESULTS**
77 **Adipocyte PI3Kα is dispensable for adipostasis and metabolic homeostasis in mice**
78 It has been proposed that PI3Kα is the main PI3K catalytic isoform in adipocyte insulin
79 signaling (Foukas et al., 2006; Knight et al., 2006). Therefore, we crossed PI3Kα LoxP
80 floxed mice (PI3K$\alpha^{F/F}$) (Molinaro et al., 2019) with mice expressing the Cre recombinase
81 under the control of the AdipoQ promoter to generate mice lacking PI3Kα specifically in
82 adipocytes (PI3Kα^{AdQ}). Compared to PI3K$\alpha^{F/F}$ mice, PI3Kα^{AdQ} mice showed a substantial
83 reduction of PI3Kα protein abundance in white fat pads and a trend in interscapular brown
84 fat, but not in other tissues (Figures S1A-D). Mature adipocytes purified from epididymal fat
85 pads of PI3Kα^{AdQ} mice showed almost complete ablation of the PI3Kα protein without
86 changes in the abundance of other catalytic or regulatory PI3K subunits or IRS1 and IRS2
87 (Figures S1E and F). PI3Kα protein abundance was not affected in adipose tissue stromal
88 vascular cells of PI3Kα^{AdQ} mice (Figures S1G and H). Thus, PI3Kα protein was almost
89 completely ablated in adipocytes of PI3Kα^{AdQ} mice but was comparable in abundance to
90 control mice in adipose stromal vascular cells, muscle, liver, kidney, brain, and spleen
91 (Figure S1).
92 PI3Kα^{AdQ} mice showed a normal growth curve, slightly reduced serum FFA levels, normal
93 fasting glucose and insulin levels, normal glucose and insulin tolerance, and normal
94 suppression of serum FFA levels by glucose (Figures 1A-C and S2A-C). Fat pad weights
95 and adipocyte size distribution of PI3Kα^{AdQ} mice were similar to controls, and their liver
96 histology was normal (Figures 1D-F and S2D). Therefore, in stark contrast with the
97 phenotype of mice lacking InsR or AKT1 and AKT2 in their adipocytes (Boucher et al., 2016;
98 Qiang et al., 2016; Sakaguchi et al., 2017; Shearin et al., 2016), PI3Kα^{AdQ} mice are not
99 lipodystrophic but show normal adiposity, glucose, and lipid homeostasis. These results
100 show that PI3Kα is functionally redundant with another PI3K isoform for insulin-PI3K-AKT
101 signaling within the adipocyte.
102
103 **Adipocyte PI3K-AKT signaling depends on PI3Kα and PI3Kβ functional redundancy**

104 To identify the PI3K isoforms driving AKT phosphorylation in the adipocyte, PI3K$\alpha^{F/F}$ mice
105 and PI3Kα^{AdQ} mice were fasted for 12 hours and received one intraperitoneal injection (i.p.)
106 of 2 g/kg of glucose in the presence of different isoform-selective PI3K inhibitors or vehicle.
107 Ten minutes after the injection, the mice were sacrificed, and the epididymal fat pads were
108 collected to measure AKT phosphorylation. AKT phosphorylation was similar in the adipose
109 tissues of PI3K$\alpha^{F/F}$ mice and PI3Kα^{AdQ} mice injected with glucose and vehicle (Figure 1G).
110 This demonstrates that, in adipocyte insulin-PI3K-AKT signaling, PI3Kα is functionally
111 redundant with another PI3K isoform. The PI3Kγ-selective inhibitor IPI549 or the PI3Kδ-
112 selective inhibitor PIK294 did not affect AKT phosphorylation in the adipose tissues of
113 PI3Kα^{AdQ} mice. Thereby PI3Kγ and PI3Kδ activities are dispensable for insulin-PI3K-AKT
114 signaling in adipocytes of PI3Kα^{AdQ} mice. However, two different PI3Kβ-selective inhibitors
115 (TGX221 and GSK2636771) substantially reduced AKT phosphorylation in the adipose
116 tissue of PI3Kα^{AdQ} mice, with GSK2636771 achieving more than 90% inhibition (Figure 1G).
117 The PI3Kβ-selective inhibitors TGX221 and GSK2636771 had no significant effect on
118 adipose tissue AKT phosphorylation in PI3K$\alpha^{F/F}$ control mice (Figure 1H). Hence, AKT
119 phosphorylation is not affected in cells with either a functional PI3Kα or PI3Kβ but it is
120 blocked in adipocytes with inactivation of both PI3Kα and PI3Kβ.
121 These results demonstrate that insulin-PI3K-AKT signaling in the mouse adipocyte,
122 in vivo, depends on functionally redundant PI3Kα and PI3Kβ activities.
123
124 **Adipocyte PI3K links adipostasis with insulin secretion**
125 Our results are consistent with previous studies showing that PI3Kβ-selective inhibition does
126 not interfere with insulin signaling (Foukas et al., 2006; Knight et al., 2006; Molinaro et al.,
127 2019; Sopasakis et al., 2010). However, the results described above demonstrate that PI3K-
128 AKT signaling can be inhibited acutely in adipocytes in vivo by administering a PI3Kβ-
129 selective inhibitor to PI3Kα^{AdQ} mice (Figures 1G, H). An adipocyte-selective acute inhibition
130 of PI3K signaling solves the problem of the lipoatrophy associated with genetic blockage of
131 adipocyte InsR-PI3K-AKT signaling in mice (Boucher et al., 2016; Qiang et al., 2016;
132 Sakaguchi et al., 2017; Shearin et al., 2016). Thus, we used this acute approach to
133 investigate the role of adipose tissue PI3K signaling in the feedback control of insulin
134 secretion. PI3K$\alpha^{F/F}$ mice and PI3Kα^{AdQ} mice were fasted for 12 hours and received one
135 intraperitoneal injection of 2 g/kg of glucose with either vehicle or the PI3Kβ-selective
136 inhibitor GSK2636771. The experiment is acute and lasted 180 minutes from the injection,
137 and the timepoint 0 minutes was just before the GSK2636771 injection. Blood glucose levels
138 were similar between groups, and serum FFA levels were significantly reduced following the

139 glucose injection in all the groups except for the PI3Kα^{AdQ} mice treated with the PI3Kβ-
140 selective inhibitor GSK2636771, where serum FFA abundance was substantially increased
141 (Figures 2A and B). Serum insulin and C-peptide (a marker for insulin secretion) were close
142 to basal levels in all groups except for PI3Kα^{AdQ} mice treated with GSK2636771, where
143 insulin secretion within 30 minutes was potently induced in a sustained manner (Fig. 2C and
144 D). These findings reveal that low adipocyte PI3K activity triggers a feedback signal that
145 potently induces insulin secretion. By analogy to the glucoincretin effect (Holst, 2019;
146 Rehfeld, 2018), we named this phenomenon "the adipoincretin effect." A similar, although
147 less potent, effect was observed in PI3Kα^{AdQ} mice treated with the PI3Kβ-selective inhibitor
148 TGX221 (Figures S3A-C). TGX221, which was less effective than GSK2636771 in reducing
149 AKT phosphorylation in adipocytes of PI3Kα^{AdQ} mice (Figure 1G), blocked the action of
150 glucose on FFA suppression but did not increase FFA above basal levels (Figure S3B).
151 Hence, the adipoincretin effect can partially be dissociated from increased serum FFA.
152 The PI3Kβ-selective inhibitors TGX221 and GSK2636771 did not affect insulin
153 secretion in cultured islets from PI3K$\alpha^{F/F}$ mice or PI3Kα^{AdQ} mice, which excludes a direct
154 effect of PI3Kβ inhibition in islet cells on insulin secretion (Figure S3D).
155 To evaluate the efficacy of adipose tissue PI3K inhibition, a cohort of mice was sacrificed
156 one hour after the GSK2636771 injection, and AKT phosphorylation was measured in
157 different tissues. Since insulin-PI3K signaling reduces cAMP-PKA signaling in adipocytes
158 (Solinas and Becattini, 2022), we have also measured the phosphorylation of hormone-
159 sensitive lipase (HSL) at PKA and AMPK sites in adipose tissues of PI3Kα^{AdQ} mice and
160 control mice. GSK2636771 showed no effect on AKT or ERK phosphorylation in PI3K$\alpha^{F/F}$
161 mice but substantially reduced AKT phosphorylation, without affecting ERK phosphorylation,
162 in the adipose tissues of PI3Kα^{AdQ} mice (Figures 2E, F, and S4). We observed increased
163 AKT Ser-473 phosphorylation in the liver and muscle of PI3Kα^{AdQ} mice treated with
164 GSK2636771 (Figures 2G and H), which is coherent with an adipose-specific PI3K inhibition
165 and the increased insulin levels observed in these mice.
166 HSL phosphorylation at the PKA sites serine 660 and 563 was also significantly increased in
167 the adipose tissues of PI3Kα^{AdQ} mice injected with GSK2636771 but not in control mice,
168 whereas HSL phosphorylation at the AMPK site serine 565 was not altered (Figures 2E and
169 F). In brown adipose tissue of PI3Kα^{AdQ} mice, GSK2636771 did not affect AKT
170 phosphorylation but increased HSL phosphorylation at PKA sites (Figures S4E and F).
171
172 Overall, PI3Kβ-selective inhibition does not interfere with insulin signaling in cells
173 expressing PI3Kα (e.g. muscle and liver), but selectively blocks AKT phosphorylation in
174 adipocytes of PI3Kα^{AdQ} mice, where PI3Kα has been genetically ablated. This approach,

175 which does not cause the severe lipoatrophy associated with genetic blockage of insulin-
176 PI3K-AKT signaling in the adipocyte (Boucher et al., 2016; Qiang et al., 2016; Sakaguchi et
177 al., 2017; Shearin et al., 2016), led us to discover that adipocyte PI3K signaling links insulin
178 secretion with adipostasis through the adipoincretin effect.
179
180 **The adipoincretin effect is independent of glucose administration or feeding**
181 Adipocyte-selective PI3K inhibition caused a potent and sustained insulin secretion, whereas
182 an intraperitoneal injection of 2 g/kg of glucose in control mice did not cause an appreciable
183 increase in serum insulin after 30 minutes from glucose administration (Figures 2A and C,
184 D). This observation demonstrates that the adipoincretin effect cannot be fully explained by
185 a rise in blood glucose. Therefore, we tested if the adipoincretin effect can be induced
186 without administering the glucose injection in fed and fasting conditions.
187 Injection of GSK2636771, without glucose, significantly increased serum FFA and induced
188 insulin secretion specifically in PI3Kα^{AdQ} mice but not in littermate control PI3K$\alpha^{F/F}$ mice, in
189 either fed conditions (Figures 3A-D) or after overnight fasting (Figures 3E-G).
190 The results in fasting conditions are particularly remarkable as in PI3Kα^{AdQ} mice starved
191 overnight, serum insulin kept increasing after GSK2636771 injection despite blood glucose
192 abundance being low and decreasing during the experiment (Figures 3E-G). One mouse
193 showed 0.43 ng/ml of insulin and 6.1 mmol/l of glucose before injection and 4.3 ng/ml of
194 insulin and 2.5 mmol/l of glucose 180 minutes post-injection. The fact that the adipoincretin
195 effect can operate in hypoglycemic mice with decreasing blood glucose, demonstrates that
196 the adipoincretin effect is not driven by increased blood glucose. By contrast, we have found
197 a strong linear correlation between the area under the curve (AUC) of serum FFA and serum
198 insulin, showing that the adipoincretin effect is closely associated with lipolysis (Figure 3H).
199 Leptin is an insulin-regulated adipokine (Saladin et al., 1995), which controls
200 adipostasis and insulin secretion (Coleman and Hummel, 1974; Covey et al., 2006).
201 Therefore, we measured serum leptin levels in PI3K$\alpha^{F/F}$ and PI3Kα^{AdQ} fasted mice after
202 GSK2636771 injection. Compared to PI3K$\alpha^{F/F}$ mice, PI3Kα^{AdQ} mice showed reduced leptin
203 levels (Figure 3I). However, this difference in serum leptin was significant only 180 minutes
204 after the GSK2636771 injection, indicating that the adipoincretin effect is not initiated by
205 reduced serum leptin.
206 To further learn about the dynamic of PI3K inhibition, we have measured adipose tissue AKT
207 phosphorylation at late time points, 120 and 180 minutes after GSK2636771 injection in
208 fasted PI3Kα^{AdQ} mice. The results show a sustained inhibition of AKT phosphorylation
209 (Figures 3J and K).

We conclude that the adipoincretin effect operates in fed and fasting conditions over a broad range of blood glucose concentrations, it is not initiated by reduced serum leptin and is associated with reduced adipocyte PI3K-AKT signaling and increased FFA.

The adipoincretin effect is not associated with glucogenic or insulinogenic amino acids or exacerbated glucose counterregulatory response

We have measured the abundances of gluconeogenic and insulinogenic amino acids by ultra-performance liquid chromatography (UPLC) coupled with mass spectroscopy (MS), and of the hormones implicated in the glucose counterregulatory response by ELISA. PI3Kα^{AdQ} mice and littermate control PI3K$\alpha^{F/F}$ mice were fasted overnight and sacrificed 90 minutes after the GSK2636771 injection. Plasma was collected at time point 0 (before injection) and 90 minutes post-injection. As expected, GSK2636771 markedly increased plasma C-peptide in PI3Kα^{AdQ} mice but not in control PI3K$\alpha^{F/F}$ mice (Figure 4A). Blood glucose was slightly reduced during the experiment to a similar extent in the two genotypes (Figure 4B). PI3Kα^{AdQ} mice and littermate control PI3K$\alpha^{F/F}$ mice also showed similar abundances of all the amino acids tested (Figure 4C). The plasma concentrations of adrenaline and corticosterone were increased during the experiment, which is consistent with a stress response to the experimental manipulation. However, plasma concentrations of adrenaline and corticosterone were virtually identical in PI3Kα^{AdQ} mice and PI3K$\alpha^{F/F}$ control mice (Figures 4D and E). We have observed a trend for glucagon to increase in PI3Kα^{AdQ} mice at 90 minutes, but this trend was quantitatively marginal and statistically not significant (Figure 4F). Growth hormone was undetectable in plasma during the experiments (Figure 4G), which is consistent with a recent study showing that growth hormone levels are drastically reduced in mice fasted overnight (de Sousa et al., 2023).

Overall, the adipoincretin effect was not associated with an increased abundance of gluconeogenic or insulinogenic amino acids or with hormones mediating the glucose counterregulatory response.

The adipoincretin effect is associated with reduced plasma BCAA and increased 3OH-4C-carnitine

We have investigated the role of candidate adipokines and metabolites in the adipoincretin effect. PI3K$\alpha^{F/F}$ mice and PI3Kα^{AdQ} mice were fasted overnight and sacrificed 30 or 90 minutes after the GSK2636771 injection. Compared to baseline levels, plasma abundance of C-peptide was substantially increased 30 and 90 minutes after GSK2636771 injection in PI3Kα^{AdQ} mice but not in PI3K$\alpha^{F/F}$ control mice (Figures 5A and S5A). Blood glucose levels were similar in PI3K$\alpha^{F/F}$ and PI3Kα^{AdQ} mice 30 minutes after GSK2636771 injection and

246 slightly, but significantly, reduced in PI3Kα^{AdQ} mice 90 minutes after GSK2636771 injection
247 (Figures 5B and S5B). We measured plasma abundances of the adipokines Adipsin,
248 FABP4, and Asprosin, which have been implicated in the control of fasting plasma insulin
249 (Lo et al., 2014; Romere et al., 2016; Scheja et al., 1999). The plasma abundances of these
250 adipokines were similar in PI3K$\alpha^{F/F}$ and PI3Kα^{AdQ} mice at 30 and 90 minutes after
251 GSK2636771 (Figure S6).
252 The branched-chain amino acid (BCAA) leucine, in combination with glutamine,
253 potently induces insulin secretion in cultured β-cells (Sener and Malaisse, 1980). PI3K$\alpha^{F/F}$
254 and PI3Kα^{AdQ} mice showed similar plasma glutamine levels at all time points. Still, plasma
255 BCAA abundances were significantly reduced in PI3Kα^{AdQ} mice compared to PI3K$\alpha^{F/F}$
256 control mice 90 minutes after GSK2636771 injection (Figures 5C, D and S5C, D). Plasma
257 abundances of branched-chain ketoacids (BCKA) were virtually identical in PI3K$\alpha^{F/F}$ and
258 PI3Kα^{AdQ} mice (Figures 5E and S5E).
259 To further learn about the effects of adipocyte PI3K inhibition on fatty acids
260 metabolism, we measured the abundance of acyl-carnitines in the plasma of the mice
261 above. Compared to control PI3K$\alpha^{F/F}$ mice, PI3Kα^{AdQ} mice showed an increased abundance
262 of plasma 3-hydroxybutyrylcarnitine (3OH-4C-Carnitine) 90 minutes after GSK2636771
263 injection (Figure 5F). Other acylcarnitines and free carnitine were not significantly altered
264 (Figures 5F and S5F).
265 These results indicate that the adipoincretin effect is not associated with increased plasma
266 abundances of Adipsin, FABP4, Asprosin, glutamine, or BCKA but is associated with
267 reduced BCAA and increased 3OH-4C-Carnitine.
268
269 **Contribution of lipolysis and FFA to the adipoincretin effect**
270 β-adrenergic agonists induce lipolysis and stimulate insulin secretion in-vivo (Imura et al.,
271 1971; Porte, 1967; Sennitt et al., 1985), whereas inhibition of lipolysis with nicotinic acid
272 (NA) reduces insulin secretion in fasting (Balasse and Ooms, 1973; Boden et al., 1998;
273 Dobbins et al., 1998a; Dobbins et al., 1998b; Stein et al., 1996).
274 To investigate the role of lipolysis in the adipoincretin effect, PI3Kα^{AdQ} mice were fasted
275 overnight and injected with 6 mg/kg of GSK2636771 alone or GSK2636771 with 56 mg/kg of
276 the adipose tissue triglyceride lipase (ATGL) inhibitor Atglistatin. As expected, GSK2636771
277 markedly increased insulin secretion over the baseline of PI3Kα^{AdQ} mice. However,
278 Atglistatin cotreatment significantly reduced the effects of GSK2636771 on serum FFA and
279 insulin secretion in PI3Kα^{AdQ} mice (Figures 6A-F). Notably, the Atglistatin treatment was
280 associated with a trend toward increased blood glucose (Figures 6A and E). However, the

281 AUC of serum insulin did not show a linear correlation with the AUC of blood glucose or of
282 FFA (Figures 6G and H).
283 We next investigated the effects of nicotinic acid (NA), which inhibits lipolysis by
284 reducing cAMP in adipocytes, on the adipoincretin effect. PI3Kα^{AdQ} mice were fasted
285 overnight and injected with either 6 mg/kg of GSK2636771 alone or GSK2636771 with 100
286 mg/kg of NA. Blood glucose levels were similar between groups and decreased during the
287 experiment (Figure 6I). Serum FFA abundance was increased over the baseline by
288 GSK2636771, but this increase was completely blocked by the NA cotreatment (Figure 6J).
289 GSK2636771 increased serum insulin levels in PI3Kα^{AdQ} mice cotreated with NA (Figure
290 6K). We observed a substantial trend, although not statistically significant, toward a reduced
291 adipoincretin effect in PI3Kα^{AdQ} mice treated with GSK2636771 in the presence of NA
292 (Figures 6K and L). Furthermore, AUC of serum insulin showed a significant linear
293 correlation with the AUC of serum FAA, but not of blood glucose (Figures 6O and P).
294 Overall whereas we have observed a clear association between lipolysis and the
295 adipoincretin effect, these results also indicate that the adipoincretin effect cannot be easily
296 explained by a general increase of circulating FFA alone. Indeed, Atglistatin was less
297 effective than NA in reducing serum FFA but more effective than NA in reducing serum
298 insulin (Figures 6B,C and J,K), without a correlation between the AUCs of serum FFA and
299 insulin (Figure 6H).
300 Although for the GSK2636771-NA cotreatment experiment there was a linear
301 correlation between the AUCs of serum FFA and insulin (Figure 6P), we also observed at 30
302 minutes post-injection the opposite change in serum FFA abundance (reduced) and insulin
303 secretion (increased) in PI3Kα^{AdQ} mice cotreated with GSK2636771 and NA (Figures 6J and
304 K). This finding was reproduced in an independent cohort of PI3Kα^{AdQ} mice cotreated with
305 GSK2636771 and NA, which showed an even more pronounced dissociation between
306 serum FFA and serum insulin (Figures S7A-D).
307 In conclusion, whereas these results are consistent with a functional role for
308 adipocyte lipolysis in the adipoincretin effect, also show that a general increase in circulating
309 FFA alone cannot fully explain this phenomenon and indicates that PI3K activity in the
310 adipocyte regulates another signal contributing to the adipoincretin effect (e.g. an
311 adipoincretin).
312
313 **The hyperinsulinemia induced by systemic PI3K inhibition can be reduced with NA**
314 The hyperinsulinemia associated with systemic PI3K inhibition reduces the therapeutic index
315 of PI3K inhibitors in cancer therapy (Hopkins et al., 2018; Vasan and Cantley, 2022).

316 Therefore, we have investigated the contribution of lipolysis and increased FFA to the insulin
317 secretion induced by whole-body PI3K inhibition (which also increases blood glucose).
318 Wild-type (WT) C57Bl6/J mice were fasted overnight and injected intraperitoneally with
319 Taselisib (3.5 mg/kg) with or without Atglistatin (56 mg/kg). As expected blood glucose and
320 serum FFA abundances were increased in mice treated with Taselisib. However, while the
321 cotreatment with Atglistatin partially reduced serum FFA, also markedly exacerbated
322 hyperglycemia (Figures 7A, and B). Nevertheless, compared to mice treated with Taselisib
323 only, mice cotreated Atglistatin showed reduced serum insulin during the first 60 minutes
324 after injection and similar serum insulin at later time points despite substantially higher blood
325 glucose (Figure 7C). There was no linear correlation between AUC of insulin and AUC of
326 either glucose or FFA (Figures 7D-H).
327 We have investigated the effects of NA on systemic PI3K inhibition by comparing WT
328 C57Bl6/J mice fasted overnight and injected with either 3.5 mg/kg of Taselisib alone with
329 mice injected with Taselisib and NA (100 mg/kg).
330 WT mice injected with of Taselisib alone showed increased blood glucose, serum FFA, and
331 substantially elevated serum insulin (Figures 7I-K). Cotreatment with NA completely
332 prevented the increase of serum FFA without affecting blood glucose (Figures 7I and J).
333 Taselisib increased serum insulin also in the presence of NA (Figure 7K). However, NA
334 significantly reduced the increase of serum insulin induced by Taselisib (Figure 7K). AUC of
335 serum insulin showed a linear correlation with AUC of FFA but not AUC of blood glucose.
336 These findings were reproduced in an independent cohort of mice in fasting and fed
337 conditions, with the only difference that there was a linear correlation also between the AUC
338 of insulin and blood glucose (Figures S7E-L and R, S). We tested the effects of NA also
339 with another pan-PI3K inhibitor, Buparlisib. However, at the dose tested (8 mg/kg),
340 Buparlisib caused only a modest increase in serum insulin and blood glucose without
341 increasing serum FFA (Figures S7M-O). Buparlisib NA cotreatment showed a trend toward
342 reduced insulin (Figures S7M-O). AUC of serum insulin was associated with AUC of blood
343 glucose but not FFA (Figures S7P, T).
344 In conclusion our results show that the hyperinsulinemia caused by systemic PI3K inhibition
345 can be significantly reduced by NA coadministration.
346
347 **DISCUSSION**
348 We now show that, during fasting, adipocyte lipolysis and basal insulin secretion are
349 coregulated by redundant PI3Kα and PI3Kβ activities within the adipocyte independently
350 from blood glucose through a feedback signal that we named the adipoincretin effect.
351 Our understanding of insulin-PI3K signaling in the adipocyte in-vivo has been limited
352 by the fact that genetic ablation of the InsR or AKT1 and AKT2 in mice adipocytes leads to

353 severe lipoatrophy with no functional adipose tissue left to study its physiological function
354 (Boucher et al., 2016; Qiang et al., 2016; Sakaguchi et al., 2017; Shearin et al., 2016). To
355 overcome this issue, we first discovered that adipocyte insulin signaling in mice is mediated
356 by the redundant activity of PI3Kα and PI3Kβ, and then we exploited this redundancy to
357 achieve an adipose tissue-selective pharmacological inhibition of PI3K activity. Acute
358 adipocyte-selective PI3K inhibition, achieved by administering GSK2636771 to PI3Kα^{AdQ}
359 mice, blocked the effect of glucose on lipolysis and increased serum FFA in mice fasted
360 overnight. This finding substantially advances our understanding of insulin action on
361 lipolysis, showing that adipocyte PI3K is active even after prolonged fasting to control the
362 rates of lipid mobilization.
363 Most importantly, we discovered that acute inhibition of PI3K activity in adipocytes
364 caused a substantial and sustained increase in insulin secretion. This phenomenon, the
365 adipoincretin effect, is independent of the feeding state. However, because the adipoincretin
366 effect is triggered by low adipocyte PI3K activity and is associated with elevated lipolysis, it
367 is logical to deduce that the physiological function of the adipoincretin effect is to control the
368 rate of lipid mobilization during fasting. Food-induced insulin secretion is mainly governed by
369 the action of glucoincretins in synergy with increased blood glucose and, to a lesser extent,
370 by the cephalic phase (Berthoud et al., 1981; Nauck et al., 1986). By contrast, our results
371 show that basal insulin secretion during fasting is chiefly controlled by the adipoincretin
372 effect, which is inhibited by adipocyte PI3K signaling (Figure 6Q).
373 This concept stands in stark contrast to the current paradigm of the insulin system, which
374 focuses on glycemic control and indicates that, during fasting, the insulin system operates as
375 a “cruise control” for lipolysis, a true adipostat (Figure 6Q) (Solinas and Becattini, 2023).
376 It has been reported that adipocyte insulin signaling controls hepatic glucose
377 production after prolonged fasting when liver glycogen is depleted (Perry et al., 2015;
378 Petersen and Shulman, 2018; Titchenell et al., 2017; Titchenell et al., 2016). However, our
379 data show that the adipoincretin effect can be dissociated from increased blood glucose.
380 The effect of adipocyte PI3K inhibition on insulin secretion was far more potent than the
381 effect on insulin secretion caused by an intraperitoneal injection of 2 g/kg of glucose (Figures
382 2A-B). In fasted mice, the adipoincretin effect was induced while blood glucose decreased
383 from more than six mmo/L to about three mmol/L (Figures 3E and G). Therefore, the
384 adipoincretin effect cannot be explained by an increase even transient in blood glucose.
385 Activation of lipolysis by β-adrenergic agonists is known to induce insulin secretion while
386 reducing blood glucose (Grujic et al., 1997; Imura et al., 1971; Porte, 1967; Yoshida, 1992).
387 The adipoincretin effect was clearly associated with increased lipolysis (Figure 3 E-H and
388 Figure 6). However, we could partially dissociate the adipoincretin effect from increased FFA

389 by co-treating PI3Kα^{AdQ} mice with the PI3Kβ-selective inhibitor GSK2636771 in the presence
390 of NA or by using the less potent PI3Kβ-selective inhibitor TGX221 (Figures S3A-B and
391 S7A-D). This observation is consistent with studies showing that increasing circulating FFA
392 by intralipids and heparin infusion does not substantially increase insulin secretion (Amery et
393 al., 2000; Balent et al., 2002; Becattini et al., 2023; Grujic et al., 1997; Hargreaves et al.,
394 1991; Schenk et al., 2005; Smiles et al., 2019; Yoshida, 1992). Atglistatin showed a more
395 pronounced inhibition of the adipoincretin effect than NA despite a partial reduction of FFA,
396 and without correlation between FFA AUC and insulin AUC (Figure 6). Finally 30 minutes
397 after NA injection serum insulin was increased while serum FFA were reduced (Figures 6J,
398 K and S7B, C).
399 Collectively, these pieces of evidence indicate that a general increase of serum FFA alone is
400 not sufficient to fully explain the adipoincretin effect, which likely depends on a specific
401 adipocyte-derived "adipoincretin" hormone whose release is controlled by PI3K activity.
402 Our data exclude a role for altered amino acid metabolism. Specific adipokines could
403 mediate the glucoincretin effect, and leptin is a logical candidate (Ahima et al., 1996;
404 Coleman and Hummel, 1974; Covey et al., 2006; D'Souza A et al., 2016; Saladin et al.,
405 1995; Trayhurn et al., 1995). Compared to control mice, mice with adipocyte-selective PI3K
406 inhibition showed reduced serum leptin, but this difference was significant only by the end of
407 the experiment, after the induction of insulin secretion (Figure 3). We conclude that the
408 adipoincretin effect is not initiated by the reduced abundance of circulating leptin. However,
409 low circulating leptin abundance likely drives insulin secretion after a prolonged period of
410 starvation when the adipose tissue is progressively depleted. This view is supported by a
411 study showing that inducible ablation of the insulin receptor in adipocytes of adult mice
412 within a few days causes severe lipoatrophy and hypoleptinemia in association with
413 hyperinsulinemia, which can be prevented by continuous leptin infusion (Sakaguchi et al.,
414 2017).
415 We investigated other candidates "adipoincretins": Adipsin, FABP4, and Asprosin (Lo et al.,
416 2014; Romere et al., 2016; Scheja et al., 1999). Adipocyte-specific PI3K inhibition did not
417 affect the circulating levels of Adipsin, FABP4, and Asprosin. However, it remains to be
418 found whether adipocyte PI3K signaling plays a role in controlling the activity of one or more
419 of these adipokines.
420 We have found that the plasma abundance of 3OH-4C-Carnitine was significantly elevated
421 in mice 90 minutes after adipocyte-selective PI3K inhibition. 3OH-4C-Carnitine is elevated in
422 humans affected by a form of hyperinsulinism caused by loss of function mutations on the
423 gene encoding for L-3-hydroxyacyl-CoA-dehydrogenase (HADH) (Clayton et al., 2001).
424 However, the role of adipocyte HADH activity in insulin secretion remains unresolved, and

more research is needed to understand the significance of increased 3OH-4C-Carnitine on insulin secretion. Some insight may be derived from our data on ATGL inhibition. The fact that Atglistatin was more effective in reducing the adipoincretin effect than NA, without showing a linear correlation between AUCs of serum insulin and FFA suggests that the adipoincretin effect may depend on a specific enzymatic activity of ATGL. Indeed, besides its lipase activity, ATGL was implicated in the synthesis of branched fatty acid esters of hydroxy fatty acids (FAHFAs) (Patel et al., 2022). Further research in this direction is granted.

The hyperinsulinemia induced by PI3K inhibitors dampens the efficacy of PI3K-targeted cancer therapy (Vasan and Cantley, 2022). We now show that inhibition of PI3K in adipocytes induces insulin secretion independently from blood glucose and that NA significantly reduces the hyperinsulinemia induced by the pan PI3K inhibitor Taselisib. Future research will test whether NA (vitamin B_3) supplementation can improve the efficacy of PI3K inhibitors in cancer therapies.

It has been proposed that in obese subjects with normal glucose tolerance, hyperinsulinemia can be explained mainly by increased baseline insulin secretion at fasting (Polonsky et al., 1988). Because adipose tissue lipolysis and fasting serum insulin are associated in obese subjects (Fryk et al., 2021), the development of hyperinsulinemia and insulin resistance in obesity may be driven by an exacerbated adipoincretin effect due to increased fat mass.

Future research on the adipoincretin effect holds great promise for developing targeted therapies for cancer, obesity, and type-2 diabetes.

Limitations of the study

The lack of identification of the specific adipoincretin endocrine signals is the major limitation of our study. However, this limitation does not make the discovery of the adipoincretin effect any less solid or disruptive. By analogy, the finding that GLP-1 is a glucoincretin was published 23 years after demonstrating the glucoincretin effect, a disruptive discovery that transformed our understanding of how food induces insulin secretion (Rehfeld, 2018). The discovery of the adipoincretin effect transforms our understanding of how the insulin system operates, revealing that during fasting, the insulin system operates as an adipostat (Figure 6Q) (Solinas and Becattini, 2023). This model has a major impact on obesity, diabetes, and cancer research.

ACKNOWLEDGMENTS

We are grateful to Prof. Claes Wollheim at Lund University for our conversations on β-cell biology and to Prof. Paolo De Los Rios at the EPFL for our conversations on the properties

of feedback control systems. This study is supported by grants from the Novo Nordisk Foundation NNF19OC0057174; the Swedish Research Council 2022-01033; the Cancerfonden 20 0840 PjF; and the Diabetesfonden DIA2022-753 to G.S.

AUTHOR CONTRIBUTIONS

B.B codesigned and performed most experiments, interpreted data, and contributed to writing the manuscript; A.M generated the PI3Kα^{AdQ} mice and characterized the PI3Kα deletion; M.H. and J.B. performed targeted metabolomics; G.S. conceived the study, analyzed, and interpreted the results, and wrote the first version of the manuscript. All authors have read and approved the manuscript.

DECLARATION OF INTERESTS

The authors declare that they have no competing interests.

Figure 1. Adipocyte AKT signaling in-vivo depends on PI3Kα and PI3Kβ.

(A) Growth curves of PI3Kα^{AdQ} and PI3K$\alpha^{F/F}$ mice. (B) Fed serum free fatty acids (FFA) of the mice above. (C) Fasting serum FFA, fasting blood glucose, and fasting serum insulin of PI3Kα^{AdQ} and PI3K$\alpha^{F/F}$ mice. (D) Adipose tissue weights of PI3Kα^{AdQ} and PI3K$\alpha^{F/F}$ mice. (E-F) Adipocyte size distribution and representative histology of epidydimal fat pads. (G) In-vivo pharmacological mapping of the PI3K isoforms driving AKT signaling in the adipocyte of PI3Kα^{AdQ} and PI3K$\alpha^{F/F}$ mice fasted for 12 hours and sacrificed 10 minutes after i.p. injection of 2 g/Kg of glucose with either vehicle or the indicated PI3K inhibitor: 6 mg/Kg for TGX221 (PI3Kβ), IPI549 (PI3Kγ), GSK2636771 (PI3Kβ), 12 mg/Kg for PIK294 (PI3Kδ). (H) The effect of the PI3Kβ-selective inhibitors TGX221 and GSK2636771 on AKT phosphorylation was evaluated in PI3K$\alpha^{F/F}$ control mice. Scale bar 100 μm for F. n=7 mice PI3K$\alpha^{F/F}$ and n=6 mice PI3Kα^{AdQ} for A-D, n=6 mice for E and F, 3 mice for G and H. Data are mean ± s.e.m. Statistical analysis was performed using Mann-Whitney for C or unpaired t-test for G.

Figure 2. Adipocyte PI3K activity links adipostasis with insulin secretion through an adipoincretin effect.

(A) Blood glucose was measured in PI3Kα^{AdQ} and PI3K$\alpha^{F/F}$ mice fasted overnight for 12 hours and injected i.p. with 2 g/Kg of glucose with either vehicle or 6 mg/Kg of the PI3Kβ-selective inhibitor GSK2636771. (B) Serum FFA; (C) serum insulin; and (D) serum C-peptide of the mice from A.

(E, F) immunoblot analysis of AKT and HSL phosphorylation in epididymal adipose tissue from mice as from A one-hour post-injection.

(G, H) immunoblot analysis of AKT phosphorylation in liver and muscle from mice as from A one-hour post-injection.

n=6 for A-D, n=2-5 for E, G (2 for fasting), n=5 for F, H. Data are represented as mean ± s.e.m. Statistical analysis was performed using repeated measures two-way ANOVA and Šídák's multiple comparisons test for A-D, and Mann-Whitney for F,H. Indicated P-values in B-D are the most conservative for PI3Kα^{AdQ} + Glucose + GSK2636771 vs PI3Kα^{AdQ} +Glucose, or vs PI3K$\alpha^{F/F}$ + Glucose + GSK2636771.

Figure 3. The adipoincretin effect operates in fed and fasted mice independently from glucose administration.

(A) Blood glucose of fed PI3Kα^{AdQ} and PI3K$\alpha^{F/F}$ mice injected with 6 mg/Kg of GSK2636771. (B) Serum levels of FFA; (C) serum insulin; and (D) serum C-peptide of the mice from A.

512 (E) Blood glucose of mice as from A but injected with 6 mg/Kg of GSK2636771 after 12
513 hours of fasting. (F) Serum levels of FFA; and (G) serum insulin of the mice from E. (H)
514 Simple linear regression of area under the curves (AUC) of insulin vs FFA; and (I) leptin of
515 the mice from E.
516 (J) Immunoblot analysis of AKT phosphorylation in epididymal adipose tissue from PI3Kα^{AdQ}
517 mice fasted for 12 hours and sacrificed 120 and 180 minutes after injection of 6 mg/Kg of
518 GSK2636771. n=5 mice for A-D and n=6 mice for E-I, n=3 for J. Data are mean ± s.e.m.
519 Statistical analysis was performed using repeated measures, two-way ANOVA for A-J,
520 Šídák's multiple comparisons test for A-G, and unpaired t-test for H.
521
522 **Figure 4. Amino acids and counterregulatory hormones in the adipoincretin effect**
523 (A) Plasma abundance of C-peptide in 12 hours fasted PI3Kα^{AdQ} and PI3K$\alpha^{F/F}$ mice 90
524 minutes after injection of 6 mg/kg of GSK2636771. (B) Blood glucose of the mice in A. (C)
525 plasma abundance of different gluconeogenic and insulinogenic amino acids.
526 Plasma levels of (D) adrenaline, (E) corticosterone, (F) glucagon, and (G) growth hormone
527 were measured by ELISA. n= 8 mice. Data are mean ± s.e.m. Statistical analysis was
528 performed using repeated measures two-way ANOVA.
529
530
531 **Figure 5. The adipoincretin effect is associated with reduced BCAA and increased**
532 **3OH-4C-Carnitine.**
533 (A) Plasma abundance of C-peptide in 12 hours fasted PI3Kα^{AdQ} and PI3K$\alpha^{F/F}$ mice after
534 injection of 6 mg/kg of GSK2636771. (B) Blood glucose of the mice in A. (C) Plasma
535 abundance of glutamine; (D) branched-chain amino acids (BCAA) and (E) branched-chain
536 ketoacids (BCKA) from the mice in A. (F) Plasma levels of free carnitine and acyl-carnitines
537 in the mice from above. n= 10 mice. Data are mean ± s.e.m. Statistical analysis was
538 performed using repeated measures two-way ANOVA and Šídák's multiple comparisons test
539 for B.
540
541 **Figure 6. Contribution of lipolysis and FFA to the adipoincretin effect**.
542 (A) Blood glucose of 12 hours fasted PI3Kα^{AdQ} mice after injection of 6 mg/kg of
543 GSK2636771 in the presence or absence of 56 mg/kg of Atglistatin. (B) The abundance of
544 serum FFA and of (C) serum insulin from the mice in A. (D) area under the curve (AUC) of
545 serum insulin in C. (E) AUC of fasting blood glucose levels in A; (F) AUC of FFA levels in B.
546 (G) Simple linear regression of AUCs of insulin vs glucose; (H) Simple linear regression of
547 AUCs of insulin vs FFA.

548 (I) Blood glucose of 12 hours fasted PI3Kα^{AdQ} mice after injection of 6 mg/kg of
549 GSK2636771 in the presence or absence of 100 mg/kg of nicotinic acid. (J) Serum FFA and
550 (K) serum insulin from the mice above. (L) AUC of fasting insulin from K. (M) AUC of fasting
551 blood glucose levels in I; (N) AUC of FFA levels in J. (O) Simple linear regression of the
552 AUCs of insulin vs glucose.
553 (P) Simple linear regression of AUCs of insulin vs FFA.
554 (Q) During feeding, insulin secretion is governed mainly by the glucoincretin effect, which
555 requires increased blood glucose. During fasting, the glucoincretin effect is absent, and
556 blood glucose concentrations are minimal. Our findings indicate that baseline insulin
557 secretion is mainly governed by closed-loop negative feedback mediated by insulin-PI3K
558 signaling in the adipocyte. The system can be regarded as an adipostat, a "cruise control"
559 for lipolysis where adipocyte PI3K activity links lipolysis with basal insulin secretion through
560 the adipoincretin effect.
561 n=6 mice for A-H, for I-P: n=6 for GSK2636771 and n=5 for GSK2636771 with NA.
562 Data are mean ± s.e.m. Statistical analysis was performed using repeated measures two-
563 way ANOVA, Šídák's multiple comparisons test, Mann-Whitney for AUC, and simple linear
564 regression for the relationship analysis of two AUC.
565
566 **Figure 7. Contribution of lipolysis to systemic PI3K inhibition**
567 (A) Blood glucose of 12 hours fasted wild-type C57Bl/6 mice after injection of 3.5 mg/kg of
568 Taselisib in the presence or absence of 56 mg/kg of Atglistatin. (B) Serum FFA and (C)
569 serum insulin from the mice above. (D) Area under the curve (AUC) of serum insulin in C.
570 (E) AUC of fasting blood glucose levels in A; (F) AUC of serum FFA in B. (G) Simple linear
571 regression of the AUCs of insulin vs glucose. (H) Simple linear regression of the AUCs of
572 insulin vs FFA.
573 (I) Blood glucose of 12 hours fasted C57Bl/6 wild-type mice after injection of 3.5 mg/kg of
574 Taselisib in the presence or absence of 100 mg/kg of nicotinic acid (NA). (J) Serum FFA and
575 (K) serum insulin from the mice above. (L) AUC of serum insulin from K. (M) AUC of fasting
576 blood glucose in I; (N) AUC of serum FFA levels in J. (O) Simple linear regression of the
577 AUCs of insulin vs glucose. (P) Simple linear regression of the AUCs of insulin vs FFA.
578 n=6 mice. Data are mean ± s.e.m. Statistical analysis was performed using repeated
579 measures two-way ANOVA, Šídák's multiple comparisons test, Mann-Whitney for AUC, and
580 simple linear regression for the relationship analysis of two AUC.
581

REFERENCES

Ahima, R.S., Prabakaran, D., Mantzoros, C., Qu, D., Lowell, B., Maratos-Flier, E., and Flier, J.S. (1996). Role of leptin in the neuroendocrine response to fasting. Nature *382*, 250-252.

Amery, C.M., Round, R.A., Smith, J.M., and Nattrass, M. (2000). Elevation of plasma fatty acids by ten-hour intralipid infusion has no effect on basal or glucose-stimulated insulin secretion in normal man. Metabolism *49*, 450-454.

Ando, Y., Inada-Inoue, M., Mitsuma, A., Yoshino, T., Ohtsu, A., Suenaga, N., Sato, M., Kakizume, T., Robson, M., Quadt, C.*, et al.* (2014). Phase I dose-escalation study of buparlisib (BKM120), an oral pan-class I PI3K inhibitor, in Japanese patients with advanced solid tumors. Cancer Sci *105*, 347-353.

Aston-Mourney, K., Wong, N., Kebede, M., Zraika, S., Balmer, L., McMahon, J.M., Fam, B.C., Favaloro, J., Proietto, J., Morahan, G.*, et al.* (2007). Increased nicotinamide nucleotide transhydrogenase levels predispose to insulin hypersecretion in a mouse strain susceptible to diabetes. Diabetologia *50*, 2476-2485.

Balasse, E.O., and Ooms, H.A. (1973). Role of plasma free fatty acids in the control of insulin secretion in man. Diabetologia *9*, 145-151.

Balent, B., Goswami, G., Goodloe, G., Rogatsky, E., Rauta, O., Nezami, R., Mints, L., Angeletti, R.H., and Stein, D.T. (2002). Acute elevation of NEFA causes hyperinsulinemia without effect on insulin secretion rate in healthy human subjects. Ann N Y Acad Sci *967*, 535-543.

Becattini, B., Molinaro, A., Henricsson, M., Borén, J., and Solinas, G. (2023). Adipocyte PI3K links adipostasis with insulin secretion through an adipoincretin effect. bioRxiv, 2023.2004.2024.538076.

Berthoud, H.R., Bereiter, D.A., Trimble, E.R., Siegel, E.G., and Jeanrenaud, B. (1981). Cephalic phase, reflex insulin secretion. Neuroanatomical and physiological characterization. Diabetologia *20 Suppl*, 393-401.

Boden, G., Chen, X., and Iqbal, N. (1998). Acute lowering of plasma fatty acids lowers basal insulin secretion in diabetic and nondiabetic subjects. Diabetes *47*, 1609-1612.

Boucher, J., Softic, S., El Ouaamari, A., Krumpoch, M.T., Kleinridders, A., Kulkarni, R.N., O'Neill, B.T., and Kahn, C.R. (2016). Differential Roles of Insulin and IGF-1 Receptors in Adipose Tissue Development and Function. Diabetes *65*, 2201-2213.

Clayton, P.T., Eaton, S., Aynsley-Green, A., Edginton, M., Hussain, K., Krywawych, S., Datta, V., Malingre, H.E., Berger, R., and van den Berg, I.E. (2001). Hyperinsulinism in short-chain L-3-hydroxyacyl-CoA dehydrogenase deficiency reveals the importance of beta-oxidation in insulin secretion. J Clin Invest *108*, 457-465.

Coleman, D.L., and Hummel, K.P. (1974). Hyperinsulinemia in pre-weaning diabetes (db) mice. Diabetologia *10 Suppl*, 607-610.

Covey, S.D., Wideman, R.D., McDonald, C., Unniappan, S., Huynh, F., Asadi, A., Speck, M., Webber, T., Chua, S.C., and Kieffer, T.J. (2006). The pancreatic beta cell is a key site for mediating the effects of leptin on glucose homeostasis. Cell Metab *4*, 291-302.

D'Souza A, M., Johnson, J.D., Clee, S.M., and Kieffer, T.J. (2016). Suppressing hyperinsulinemia prevents obesity but causes rapid onset of diabetes in leptin-deficient Lep(ob/ob) mice. Mol Metab *5*, 1103-1112.

de Sousa, M.E., Gusmao, D.O., Dos Santos, W.O., Moriya, H.T., de Lima, F.F., List, E.O., Kopchick, J.J., and Donato, J., Jr. (2023). Fasting and prolonged food restriction differentially affect GH secretion independently of GH receptor signaling in AgRP neurons. J Neuroendocrinol, e13254.

Dobbins, R.L., Chester, M.W., Daniels, M.B., McGarry, J.D., and Stein, D.T. (1998a). Circulating fatty acids are essential for efficient glucose-stimulated insulin secretion after prolonged fasting in humans. Diabetes *47*, 1613-1618.

Dobbins, R.L., Chester, M.W., Stevenson, B.E., Daniels, M.B., Stein, D.T., and McGarry, J.D. (1998b). A fatty acid- dependent step is critically important for both glucose- and non-glucose-stimulated insulin secretion. J Clin Invest *101*, 2370-2376.

636 Fergusson, G., Ethier, M., Guevremont, M., Chretien, C., Attane, C., Joly, E., Fioramonti, X.,
637 Prentki, M., Poitout, V., and Alquier, T. (2014). Defective insulin secretory response to
638 intravenous glucose in C57Bl/6J compared to C57Bl/6N mice. Mol Metab *3*, 848-854.
639 Foukas, L.C., Claret, M., Pearce, W., Okkenhaug, K., Meek, S., Peskett, E., Sancho, S.,
640 Smith, A.J., Withers, D.J., and Vanhaesebroeck, B. (2006). Critical role for the p110alpha
641 phosphoinositide-3-OH kinase in growth and metabolic regulation. Nature *441*, 366-370.
642 Fryk, E., Olausson, J., Mossberg, K., Strindberg, L., Schmelz, M., Brogren, H., Gan, L.M.,
643 Piazza, S., Provenzani, A., Becattini, B.*, et al.* (2021). Hyperinsulinemia and insulin
644 resistance in the obese may develop as part of a homeostatic response to elevated free fatty
645 acids: A mechanistic case-control and a population-based cohort study. EBioMedicine *65*,
646 103264.
647 Grujic, D., Susulic, V.S., Harper, M.E., Himms-Hagen, J., Cunningham, B.A., Corkey, B.E.,
648 and Lowell, B.B. (1997). Beta3-adrenergic receptors on white and brown adipocytes mediate
649 beta3-selective agonist-induced effects on energy expenditure, insulin secretion, and food
650 intake. A study using transgenic and gene knockout mice. J Biol Chem *272*, 17686-17693.
651 Guilherme, A., Rowland, L.A., Wang, H., and Czech, M.P. (2022). The adipocyte
652 supersystem of insulin and cAMP signaling. Trends Cell Biol.
653 Hargreaves, M., Kiens, B., and Richter, E.A. (1991). Effect of increased plasma free fatty
654 acid concentrations on muscle metabolism in exercising men. J Appl Physiol (1985) *70*, 194-
655 201.
656 Holst, J.J. (2019). From the Incretin Concept and the Discovery of GLP-1 to Today's
657 Diabetes Therapy. Front Endocrinol (Lausanne) *10*, 260.
658 Hopkins, B.D., Pauli, C., Du, X., Wang, D.G., Li, X., Wu, D., Amadiume, S.C., Goncalves,
659 M.D., Hodakoski, C., Lundquist, M.R.*, et al.* (2018). Suppression of insulin feedback
660 enhances the efficacy of PI3K inhibitors. Nature *560*, 499-503.
661 Imura, H., Kato, Y., Ikeda, M., Morimoto, M., and Yawata, M. (1971). Effect of adrenergic-
662 blocking or -stimulating agents on plasma growth hormone, immunoreactive insulin, and
663 blood free fatty acid levels in man. J Clin Invest *50*, 1069-1079.
664 Kahn, S.E., Prigeon, R.L., McCulloch, D.K., Boyko, E.J., Bergman, R.N., Schwartz, M.W.,
665 Neifing, J.L., Ward, W.K., Beard, J.C., Palmer, J.P.*, et al.* (1993). Quantification of the
666 relationship between insulin sensitivity and beta-cell function in human subjects. Evidence
667 for a hyperbolic function. Diabetes *42*, 1663-1672.
668 Kalinsky, K., Sparano, J.A., Zhong, X., Andreopoulou, E., Taback, B., Wiechmann, L.,
669 Feldman, S.M., Ananthakrishnan, P., Ahmad, A., Cremers, S.*, et al.* (2018). Pre-surgical trial
670 of the AKT inhibitor MK-2206 in patients with operable invasive breast cancer: a New York
671 Cancer Consortium trial. Clin Transl Oncol *20*, 1474-1483.
672 Knight, Z.A., Gonzalez, B., Feldman, M.E., Zunder, E.R., Goldenberg, D.D., Williams, O.,
673 Loewith, R., Stokoe, D., Balla, A., Toth, B.*, et al.* (2006). A pharmacological map of the PI3-
674 K family defines a role for p110alpha in insulin signaling. Cell *125*, 733-747.
675 Kodama, K., Tojjar, D., Yamada, S., Toda, K., Patel, C.J., and Butte, A.J. (2013). Ethnic
676 differences in the relationship between insulin sensitivity and insulin response: a systematic
677 review and meta-analysis. Diabetes Care *36*, 1789-1796.
678 Lo, J.C., Ljubicic, S., Leibiger, B., Kern, M., Leibiger, I.B., Moede, T., Kelly, M.E., Chatterjee
679 Bhowmick, D., Murano, I., Cohen, P.*, et al.* (2014). Adipsin is an adipokine that improves
680 beta cell function in diabetes. Cell *158*, 41-53.
681 Molinaro, A., Becattini, B., Mazzoli, A., Bleve, A., Radici, L., Maxvall, I., Sopasakis, V.R.,
682 Molinaro, A., Backhed, F., and Solinas, G. (2019). Insulin-Driven PI3K-AKT Signaling in the
683 Hepatocyte Is Mediated by Redundant PI3Kalpha and PI3Kbeta Activities and Is Promoted
684 by RAS. Cell Metab *29*, 1400-1409 e1405.
685 Nauck, M.A., Homberger, E., Siegel, E.G., Allen, R.C., Eaton, R.P., Ebert, R., and
686 Creutzfeldt, W. (1986). Incretin effects of increasing glucose loads in man calculated from
687 venous insulin and C-peptide responses. J Clin Endocrinol Metab *63*, 492-498.
688 Patel, R., Santoro, A., Hofer, P., Tan, D., Oberer, M., Nelson, A.T., Konduri, S., Siegel, D.,
689 Zechner, R., Saghatelian, A.*, et al.* (2022). ATGL is a biosynthetic enzyme for fatty acid
690 esters of hydroxy fatty acids. Nature *606*, 968-975.

691 Patnaik, A., Appleman, L.J., Tolcher, A.W., Papadopoulos, K.P., Beeram, M., Rasco, D.W.,
692 Weiss, G.J., Sachdev, J.C., Chadha, M., Fulk, M.*, et al.* (2016). First-in-human phase I study
693 of copanlisib (BAY 80-6946), an intravenous pan-class I phosphatidylinositol 3-kinase
694 inhibitor, in patients with advanced solid tumors and non-Hodgkin's lymphomas. Ann Oncol
695 *27*, 1928-1940.
696 Perry, R.J., Camporez, J.G., Kursawe, R., Titchenell, P.M., Zhang, D., Perry, C.J., Jurczak,
697 M.J., Abudukadier, A., Han, M.S., Zhang, X.M.*, et al.* (2015). Hepatic acetyl CoA links
698 adipose tissue inflammation to hepatic insulin resistance and type 2 diabetes. Cell *160*, 745-
699 758.
700 Petersen, M.C., and Shulman, G.I. (2018). Mechanisms of Insulin Action and Insulin
701 Resistance. Physiol Rev *98*, 2133-2223.
702 Polonsky, K.S., Given, B.D., and Van Cauter, E. (1988). Twenty-four-hour profiles and
703 pulsatile patterns of insulin secretion in normal and obese subjects. J Clin Invest *81*, 442-
704 448.
705 Porte, D., Jr. (1967). Beta adrenergic stimulation of insulin release in man. Diabetes *16*, 150-
706 155.
707 Qiang, G., Whang Kong, H., Xu, S., Pham, H.A., Parlee, S.D., Burr, A.A., Gil, V., Pang, J.,
708 Hughes, A., Gu, X.*, et al.* (2016). Lipodystrophy and severe metabolic dysfunction in mice
709 with adipose tissue-specific insulin receptor ablation. Mol Metab *5*, 480-490.
710 Rehfeld, J.F. (2018). The Origin and Understanding of the Incretin Concept. Front
711 Endocrinol (Lausanne) *9*, 387.
712 Romere, C., Duerrschmid, C., Bournat, J., Constable, P., Jain, M., Xia, F., Saha, P.K., Del
713 Solar, M., Zhu, B., York, B.*, et al.* (2016). Asprosin, a Fasting-Induced Glucogenic Protein
714 Hormone. Cell *165*, 566-579.
715 Sakaguchi, M., Fujisaka, S., Cai, W., Winnay, J.N., Konishi, M., O'Neill, B.T., Li, M., Garcia-
716 Martin, R., Takahashi, H., Hu, J.*, et al.* (2017). Adipocyte Dynamics and Reversible
717 Metabolic Syndrome in Mice with an Inducible Adipocyte-Specific Deletion of the Insulin
718 Receptor. Cell Metab *25*, 448-462.
719 Saladin, R., De Vos, P., Guerre-Millo, M., Leturque, A., Girard, J., Staels, B., and Auwerx, J.
720 (1995). Transient increase in obese gene expression after food intake or insulin
721 administration. Nature *377*, 527-529.
722 Scheja, L., Makowski, L., Uysal, K.T., Wiesbrock, S.M., Shimshek, D.R., Meyers, D.S.,
723 Morgan, M., Parker, R.A., and Hotamisligil, G.S. (1999). Altered insulin secretion associated
724 with reduced lipolytic efficiency in aP2-/- mice. Diabetes *48*, 1987-1994.
725 Schenk, S., Cook, J.N., Kaufman, A.E., and Horowitz, J.F. (2005). Postexercise insulin
726 sensitivity is not impaired after an overnight lipid infusion. Am J Physiol Endocrinol Metab
727 *288*, E519-525.
728 Sener, A., and Malaisse, W.J. (1980). L-leucine and a nonmetabolized analogue activate
729 pancreatic islet glutamate dehydrogenase. Nature *288*, 187-189.
730 Sennitt, M.V., Arch, J.R., Levy, A.L., Simson, D.L., Smith, S.A., and Cawthorne, M.A. (1985).
731 Anti-hyperglycaemic action of BRL 26830, a novel beta-adrenoceptor agonist, in mice and
732 rats. Biochem Pharmacol *34*, 1279-1285.
733 Shearin, A.L., Monks, B.R., Seale, P., and Birnbaum, M.J. (2016). Lack of AKT in adipocytes
734 causes severe lipodystrophy. Mol Metab *5*, 472-479.
735 Small, L., Ehrlich, A., Iversen, J., Ashcroft, S.P., Trost, K., Moritz, T., Hartmann, B., Holst,
736 J.J., Treebak, J.T., Zierath, J.R.*, et al.* (2022). Comparative analysis of oral and
737 intraperitoneal glucose tolerance tests in mice. Mol Metab *57*, 101440.
738 Smiles, W.J., Churchward-Venne, T.A., van Loon, L.J.C., Hawley, J.A., and Camera, D.M.
739 (2019). A single bout of strenuous exercise overcomes lipid-induced anabolic resistance to
740 protein ingestion in overweight, middle-aged men. FASEB J *33*, 7009-7017.
741 Solinas, G., and Becattini, B. (2022). PI3K and AKT at the Interface of Signaling and
742 Metabolism. Curr Top Microbiol Immunol *436*, 311-336.
743 Solinas, G., and Becattini, B. (2023). An adipoincretin effect links adipostasis with insulin
744 secretion Trends Endocrinol Metab *In press*.

745 Sopasakis, V.R., Liu, P., Suzuki, R., Kondo, T., Winnay, J., Tran, T.T., Asano, T., Smyth, G.,
746 Sajan, M.P., Farese, R.V.*, et al.* (2010). Specific roles of the p110alpha isoform of
747 phosphatidylinsositol 3-kinase in hepatic insulin signaling and metabolic regulation. Cell
748 Metab *11*, 220-230.
749 Stein, D.T., Esser, V., Stevenson, B.E., Lane, K.E., Whiteside, J.H., Daniels, M.B., Chen, S.,
750 and McGarry, J.D. (1996). Essentiality of circulating fatty acids for glucose-stimulated insulin
751 secretion in the fasted rat. J Clin Invest *97*, 2728-2735.
752 Titchenell, P.M., Lazar, M.A., and Birnbaum, M.J. (2017). Unraveling the Regulation of
753 Hepatic Metabolism by Insulin. Trends Endocrinol Metab *28*, 497-505.
754 Titchenell, P.M., Quinn, W.J., Lu, M., Chu, Q., Lu, W., Li, C., Chen, H., Monks, B.R., Chen,
755 J., Rabinowitz, J.D.*, et al.* (2016). Direct Hepatocyte Insulin Signaling Is Required for
756 Lipogenesis but Is Dispensable for the Suppression of Glucose Production. Cell Metab *23*,
757 1154-1166.
758 Trayhurn, P., Thomas, M.E., Duncan, J.S., and Rayner, D.V. (1995). Effects of fasting and
759 refeeding on ob gene expression in white adipose tissue of lean and obese (oblob) mice.
760 FEBS Lett *368*, 488-490.
761 Vasan, N., and Cantley, L.C. (2022). At a crossroads: how to translate the roles of PI3K in
762 oncogenic and metabolic signalling into improvements in cancer therapy. Nat Rev Clin Oncol
763 *19*, 471-485.
764 von Mehren, M., George, S., Heinrich, M.C., Schuetze, S.M., Yap, J.T., Yu, J.Q., Abbott, A.,
765 Litwin, S., Crowley, J., Belinsky, M.*, et al.* (2020). Linsitinib (OSI-906) for the Treatment of
766 Adult and Pediatric Wild-Type Gastrointestinal Stromal Tumors, a SARC Phase II Study.
767 Clin Cancer Res *26*, 1837-1845.
768 Yoshida, T. (1992). The antidiabetic beta 3-adrenoceptor agonist BRL 26830A works by
769 release of endogenous insulin. Am J Clin Nutr *55*, 237S-241S.

STAR★METHODS

KEY RESOURCES TABLE

REAGENT or RESOURCE	SOURCE	IDENTIFIER
Antibodies		
AKT Phospho (Thr308)	Cell Signaling	4056
AKT Phospho (Ser373) XP	Cell Signaling	4060
AKT	Cell Signaling	9272
Erk 1/2 (p44/42 MAPK) Phospho(Thr202/Tyr204) XP	Cell Signaling	9101
Erk 1/2 (p44/42 MAPK)	Cell Signaling	9102
IRS1	Millipore	06248
IRS2	Millipore	MAB515
PI3K p85	Cell Signaling	4257S
PI3K p85α	Abcam	Ab133595
PI3K p55γ	Abcam	Ab238509
Tubulin α/β	Cell Signaling	2148S
PI3Kα	Cell Signaling	4249
PI3Kβ	Cell Signaling	3011
PI3Kδ	Millipore	04-401
PI3Kγ	a gift of Prof. Matthias Wymann University of Basel	(Russian)
HSL Phospho (Ser563)	Cell Signaling	4135
HSL Phospho (Ser660)	Cell Signaling	4126
HSL Phospho (Ser565)	Cell Signaling	4137
HSL	Cell Signaling	4107
Chemicals, Peptides, Recombinant Proteins and Inhibitors		
Insulin	Humalog Lilly	VL7510
Glucose	Acros	410955000
BSA	Fisher Scientific	BP9702
ECL-anti rabbit IgG HRP	GE Healthcare	NA934V
ECL-anti mouse IgG HRP	GE Healthcare	LNA931V
Collagenase P	Roche	11213865001
GSK2636771 (Inhibitor PI3Kβ)	SelleckChem	S8002
TGX-221 (Inhibitor PI3Kβ)	MedChem Express	HY-10114
IPI549 (Inhibitor PI3Kγ)	MedChem Express(SelleckChem)	HY-100716
PIK294 (Inhibitor PI3Kδ)	MedChem Express	HY-10303
Buparlisib (BKM120, panPI3K inhibitor)	MedChem Express	HY-70063
Taselisib (GDC-0032, panPI3K inhibitor)	MedChem Express	HY-13898
Nicotinic Acid	Sigma	72309
Atglistatin	MedChem Express	HY-15859
Cremophor EL	Millipore	238470
Critical Commercial Assays		
Insulin ELISA Kit	Crystal Chem	90080

C-peptide Elisa Kit	Crystal Chem	90050
FFA (NEFA-HR set)	Fuji Film	436-91995, 434-91795 91096 (standard)
Leptin Elisa Kit	R&D	MOB00B
Adipsin Elisa Kit	R&D	DY5430-05
FABP4 Elisa Kit	BioVendor	RD191036200R
Asprosin Elisa Kit	Abbexa	abx585287
Adrenaline Elisa Kit	LDN	BA E-5100R
Corticosterone Elisa Kit	IDS	AC-14F1
Glucagon Elisa Kit	Crystal Chem	81518
Mouse Growth factor Elisa Kit	Crystal Chem	80587
Immobilon Western Chemiluminescence HRP substrate	Millipore	WBKLS0500
Hematoxylin Solution (Mayer's, Modified)	Abcam	AB220365
Eosin	Sigma	HT110116
Experimental Models: Organisms/Strains		
WT	C57BL/6 background	Janvier Labs
PI3Kα^{Flox}	Mixed background	Provided by Victoria Rotter Sopasakis
PI3Kα^{AdQ}	Mixed background	Provided by Victoria Rotter Sopasakis
Software and Algorithms		
Image Lab software (version 5.2.1)	Bio-Rad	http://www.bio-rad.com/en-us/ product/image-lab-software
Graph Pad Prism 7.0	Graph Pad Software	N/A
AxioVision Software	Imaging Sofware	Carl Zeiss Microscopy
Deposited Data		
DOI: 10.17632/tgsgkjz28w.1	Immunoblots images	N/A

CONTACT FOR REAGENT AND RESOURCE SHARING

Further information and requests for reagents may be directed to the Lead Contact, Giovanni Solinas (giovanni.solinas@wlab.gu.se)

Mice and In Vivo Studies

All mouse studies were approved by the Ethics Committee on Animal Care Use in Gothenburg, Sweden. Only male mice were used in this study. Mice were maintained at the EBM specific pathogen free facility of the University of Gothenburg under a 12-hour light /12-hour dark cycles and at a room temperature of 22°C.

PI3Kα LoxP floxed mice (PI3Kα$^{F/F}$) in 129/SvJ and C57BL/6J mixed background were previously described (Molinaro et al., 2019). PI3Kα^{AdQ} mice and littermate control PI3Kα$^{F/F}$ mice were obtained by crossing Adipoq-Cre mice in pure C57BL/6J background (Jackson labs) with the PI3Kα$^{F/F}$ mice from above. Wild-type (WT) C57BL/6J mice were obtained from Janvier Labs. For the insulin-tolerance test (ITT), mice were fasted for 4 hours and injected intraperitoneally with 1 I.U. of insulin per Kg of body weight. Blood was collected from the tail at the indicated post-injection times, and blood glucose concentrations were measured using a glucometer (Contour Next, Ascensia). For the glucose tolerance test (GTT), mice were fasted for either 4 hours (GTT in Figure S2) or overnight for glucose-mediate suppression of lipolysis (Figure 2) and injected intraperitoneally with either 1g or 2 g of glucose per Kg of body weight respectively. Blood was collected from the tail at the indicated time points and used to measure blood glucose and prepare serum to measure hormones and metabolites. For in vivo injection of PI3K inhibitors, the indicated dose of the compound was injected intraperitoneally into eight to twelve-weeks-old PI3Kα^{AdQ} mice and PI3Kα$^{F/F}$ littermate controls or C57BL/6 mice. All mice were treated acutely. For each experiment, mice were injected only once immediately after the 0-minute time point, and the experiment lasted for a maximum of 180 minutes. We used a low dose of isoform-selective PI3K inhibitors (e.g., 6 mg/Kg of body weight for GSK2636771) to ensure isoform selectivity during the relatively short time of the experiment (no longer than 180 minutes). This dose was determined in a previous study for TGX221, which we identified as the lowest dose that increased blood glucose in mice lacking PI3Kα in their hepatocytes but not in control mice (Molinaro et al., 2019). The dose of all other isoform-selective inhibitors was estimated relative to the dose of TGX221 we used and the IC_{50} of the specific PI3K inhibitor. The injectable solutions of the PI3K inhibitors were freshly prepared as follows: PI3K inhibitor was first dissolved in pure DMSO, and to this master liquid were added one by one and in this order PEG300, Tween 80, and water. The solution was mixed after each addition. The final concentration for the single components was as follows: 5% DMSO, 30% PEG, and 1% Tween-80. Control ‘‘vehicle solution’’ was 5% DMSO, 30% PEG, 1% Tween-80, and water. For solutions including Atglistatin, the latter was added to a water fraction containing 0.5% of Cremophor EL and dissolved by means of ultrasonication. The water solution thus obtained was added to the DMSO/PEG300/Tween80 mixture. For solutions including nicotinic acid (NA), the NA powder was directly dissolved in the final mix at the desired concentration; the acidity was adjusted at a value of pH 7 by adding NaOH 1M to the solution. Blood glucose was measured at the indicated time points after injection and blood was collected for further measurements of

serum insulin, serum FFA, serum leptin, and plasma levels of C-peptide, BCAA, BCKA, aminoacids, free and acyl-carnitines.
At sacrifice, mice were anesthetized with Isofluorane (Baxter KDG 9623) and euthanized by CO_2 and bleeding.

Insulin, C-peptide, Leptin, counterregulatory factors, and adipokine measurements
Insulin and C-peptide levels in serum and plasma were measured using an ELISA kit from Crystal Chem. Serum leptin was measured by ELISA kit from R&D. Counterregulatory factor adrenaline corticosterone, glucagon, and growth hormone were measured using Elisa kits from LDN, IDS, and Crystal Chem respectively. Plasma Adipsin (Mouse Complement Factor D) was measured by quantitative sandwich enzyme immunoassay using kits obtained from R&D Systems, and adipocyte FABP4 abundance in plasma was measured using an ELISA kit from BioVendor. All ELISA assays were performed according to the instruction of the manufacturer.

Hematoxylin and eosin (H&E) staining
Samples of adipose tissue pads and liver were obtained from 13-week-old mice. The samples were fixed in 10% formalin, embedded in paraffin, cut into 5 μm sections, and stained with hematoxylin (Abcam) and eosin (Sigma). H&E stained sections were imaged at 20X magnification with an AxioImager M1 microscope (Zeiss, Germany).

Adipocyte size distribution
Images of two fields for six mice were analyzed in Fiji using the open source plugin adiposoft. Cell surface area was calculated in microns and classified based on area μm^2.

Immunoblot Analysis
For analysis of protein phosphorylation, we noticed that stripping procedures frequently reduce the overall immunoblot quality and sporadically create artifacts. Thereby protein samples were loaded in parallel. For controls on total proteins, tubulin was analyzed from the same membrane when possible. resolved by SDS-PAGE electrophoresis and then transferred to a PVDF membrane. The membrane-blocking procedure was carried out at room temperature in phosphate saline buffer (PBS) with 3% bovine serum albumin (BSA), and 0.3% tween solution (Cell Metabolism 30, 1400–1409.e1–e5, June 4, 2019 e4). The primary antibody was incubated in a cold room overnight in PBS with 0.3% tween and 3% BSA; the membranes were then washed three times with a PBS 0.3% tween solution and incubated with a horseradish

peroxidase-conjugated secondary antibody (GE Healthcare) in PBS 0.3% tween 3% BSA for one hour at room temperature. After three washes in a PBS 0.3% tween solution and incubation with a detection reagent (Millipore), the signal was acquired using the Biorad ChemiDoc apparatus.

Analysis of plasma branched-chain amino acids and branched-chain keto acids

25 µl plasma and standard was precipitated with 250 µl methanol containing 1 µM of deuterated internal standards (Valine-$^{13}C_5$,^{15}N, Leucine d_3, Isoleucine d_{10}, keto-leucine d_7 and keto-isoleucine). After 10 minutes of vortex at 1400 rpm, the samples were centrifuged at 4000g for 10 minutes. 25 µl was removed and evaporated under a stream of nitrogen gas. The samples were reconstituted in 125 µl water and injected into the UPLC-MS/MS system. Separation was performed on a Waters Acquity BEH C8 column (2.1 x 100mm 1.7 µm) with a gradient consisting of water and acetonitrile, both with 0.1% formic acid. The detection was made on a Waters Xevo TQ-XS triple quadrupole mass spectrometer in MRM mode using intra-run polarity switching where the detection of amino acids was made in positive mode between 0-3 minutes. The polarity was then switched into a negative mode for the detection of the keto acids between 3-10 minutes. The standard curve containing all six amino- and keto acids was prepared in 20% methanol and treated the same way as the samples.

Analysis of plasma acylcarnitines and aminoacids

25 µl of plasma was precipitated with 250 µl of methanol containing 1 µM of stable isotope labelled internal standards ([1] Alanine-D_4, Ariginine-$^{13}C_6$ $^{15}N_5$, Glutamic acid-D_5, Glutamine-$^{13}C_5$ $^{15}N_2$, Glycine-D_5, Lysine-D_4, Methionine-$^{13}C_1$ D_3, Phenylalanine-D_8, Proline-$^{13}C_5$ $^{15}N_1$, Serine-$^{13}C_3$ D_1 $^{15}N_1$, Tryptophan-D_5). After 10 minutes of vortex at 1400 rpm, the samples were centrifuged at 4000g for 10 minutes. 25 µl was removed and evaporated under a stream of nitrogen gas. The samples were reconstituted in 125 µl of an acylcarnitine internal standard mix (NSK-B reference mix, Cambridge Isotope Laboratories) prepared in acetonitrile: methanol [3:1]. The samples were separated in HILIC mode on a Waters BEH Amide column (2.1 x 100 1.7µm) using 5 mM ammonium formate and 0.06% formic acid in 95% acetonitrile as mobile phase A and 10 mM ammonium formate and 0.12% formic acid in 100% Milli-Q water as mobile phase B. The detection was made on a Waters Xevo TQ triple quadrupole mass spectrometer in positive MRM mode. Quantification of acylcarnitines was made using a one-point calibration against the deuterated analog. For the acylcarnitines without a deuterated analog, the quantification was made against the deuterated acylcarnitine closest in retention time. Amino

acids were quantified against an external calibration curve made with reference substances in 20% methanol. For some amino acids the reference substance was missing (asparagine, glutamic acid and tyrosine). For those amino acids no quantification was made. Instead the relative amount was attained by dividing the endogenous signal with the internal standard. For amino acids that lack the labelled analogue, another internal standard (with similar retention time) was used.

Glucose Stimulated insulin secretion (GSIS)

Primary mouse islet isolation was performed as previously described (Hugill A, Shimomura K, Cox RD. Islet Insulin Secretion Measurements in the Mouse. Curr Protoc Mouse Biol. 2016 Sep 1;6(3):256-271. doi: 10.1002/cpmo.14. PMID: 27584553). After isolation and overnight incubation at 37°C with humidified 5% CO_2 air in RPMI supplemented with 1% P/S and 10% FBS, islets were transferred into a 24-well plate. 5 islets were hand-picked and transferred into each well in the presence of 200 µl low glucose buffer (Krebs Ringer Buffer KRB supplemented with 0.2% BSA and 2.8 mM glucose) and pre-incubated for 1 hour at 37°C. Islets underwent successive incubations for 20 minutes at 37°C with 200 µL of fresh KRB 0.2% BSA containing low glucose (2.8 mM), followed by high glucose (16.7 mM). At the end of each incubation, islets were transferred into a new well, and the supernatant was collected for analysis of insulin levels. At the end of the stimulation protocol, cells were lysed in 70 µL acid ethanol (75% absolute ethanol, 23.5% water, 1.5% HCl) and stored at 4°C overnight. Samples were dried with a SpeedVac and resuspended in 30 µL ultrapure water. DNA was quantified by Nanodrop (ThermoFisher, USA), and insulin was quantified using an ELISA kit (Crystal Chem) and normalized to DNA content.

QUANTIFICATION AND STATISTICAL ANALYSIS

Data are expressed as means, and error bars indicate standard errors.

Only biological replicates, defined as data from tissues of different mice, are used for statistical analysis. The exact number of mice for a specific experiment is indicated in the figure legends. For all experiments, littermate male mice with similar body weight were used.

Sample size was determined empirically based on previous experience and practical considerations. In the time course after injection, a minimum of 5 mice was used; for all other in vivo studies, a minimum of 3 biological replicates was analyzed when parametric statistical tests were used, whereas a minimum of 4 biological replicates was analyzed when non-parametric statistical tests were used. In analyses where two different categorical variables are considered

(GTT, ITT, mice weight gain, and time-course analyses), repeated measures (RM) two-way ANOVA was used. P values in the figures always refers to the group effect. The exact P values are shown when close to 0.05.

All statistical analysis was performed with GraphPad Prism software.

Figure 1

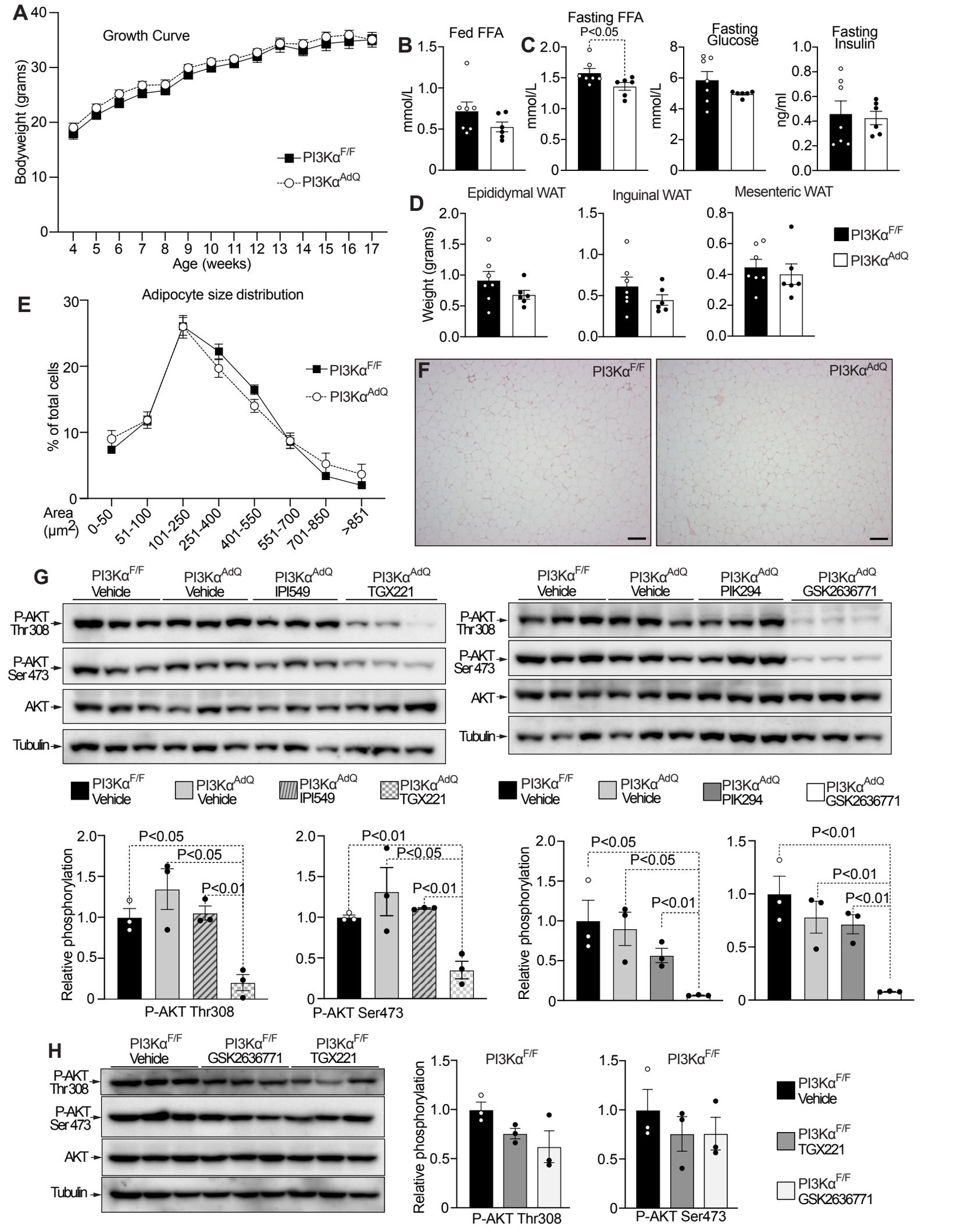
A
Growth Curve
Bodyweight (grams)
Age (weeks)
PI3Kα F/F
PI3Kα AdQ
B
Fed FFA
mmol/L
C
Fasting FFA
P<0.05
Fasting Glucose
Fasting Insulin
ng/ml
D
Epididymal WAT
Inguinal WAT
Mesenteric WAT
Weight (grams)
E
Adipocyte size distribution
% of total cells
Area (μm2)
0-50
51-100
101-250
251-400
401-550
551-700
701-850
>851
F
G
PI3Kα F/F Vehicle
PI3Kα AdQ Vehicle
PI3Kα AdQ IPI549
PI3Kα AdQ TGX221
PI3Kα AdQ PIK294
PI3Kα AdQ GSK2636771
P-AKT Thr308
P-AKT Ser473
AKT
Tubulin
Relative phosphorylation
P<0.05
P<0.01
H
PI3Kα F/F Vehicle
PI3Kα F/F GSK2636771
PI3Kα F/F TGX221

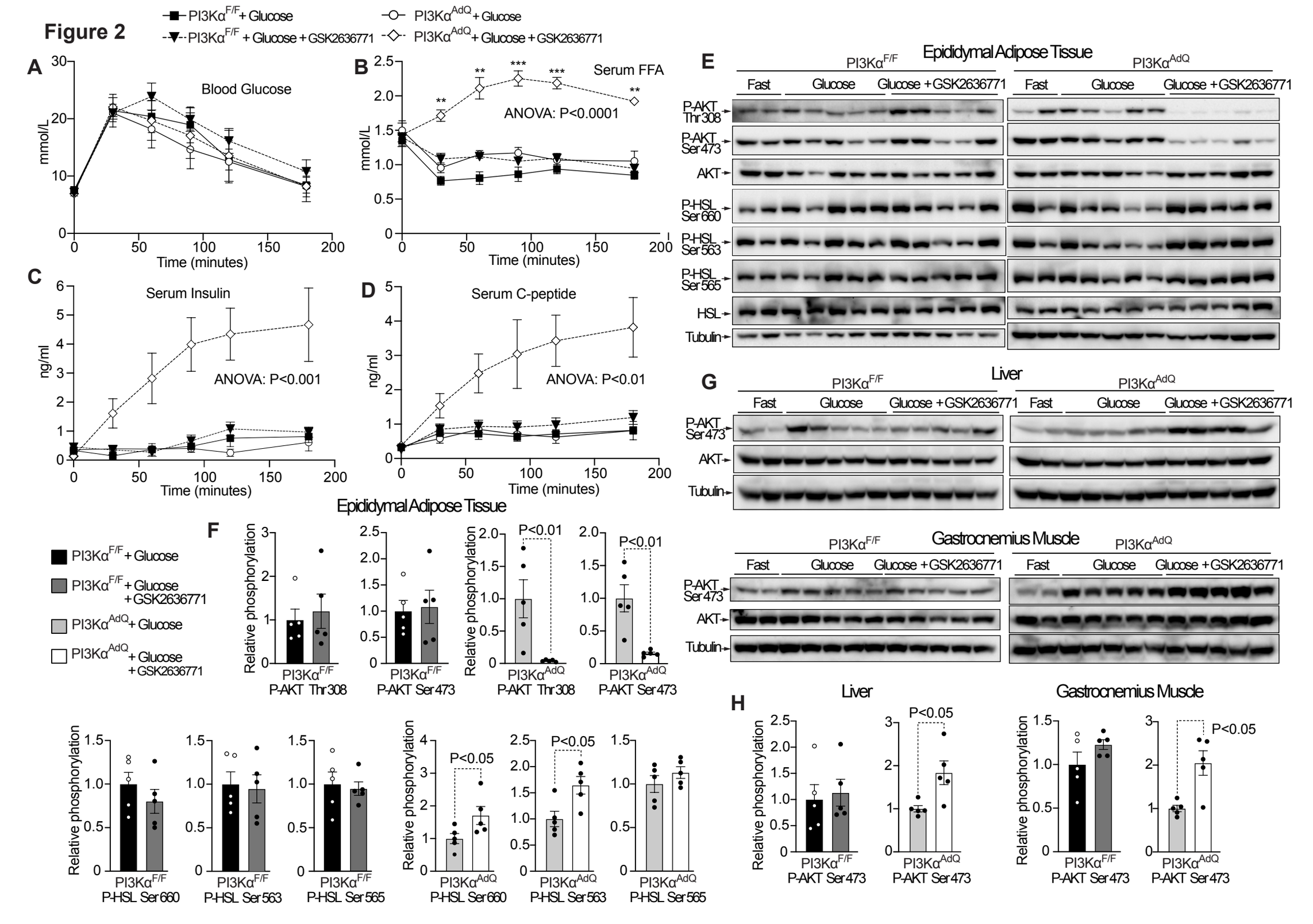
Figure 2
PI3Kα^F/F + Glucose
PI3Kα^F/F + Glucose + GSK2636771
PI3Kα^AdQ + Glucose
PI3Kα^AdQ + Glucose + GSK2636771
A
Blood Glucose
mmol/L
Time (minutes)
B
Serum FFA
ANOVA: P<0.0001
C
Serum Insulin
ANOVA: P<0.001
ng/ml
D
Serum C-peptide
ANOVA: P<0.01
E
Epididymal Adipose Tissue
Fast
Glucose
Glucose + GSK2636771
P-AKT Thr308
P-AKT Ser473
AKT
P-HSL Ser660
P-HSL Ser563
P-HSL Ser565
HSL
Tubulin
G
Liver
Gastrocnemius Muscle
F
Relative phosphorylation
P<0.01
P<0.05
H

Figure 3

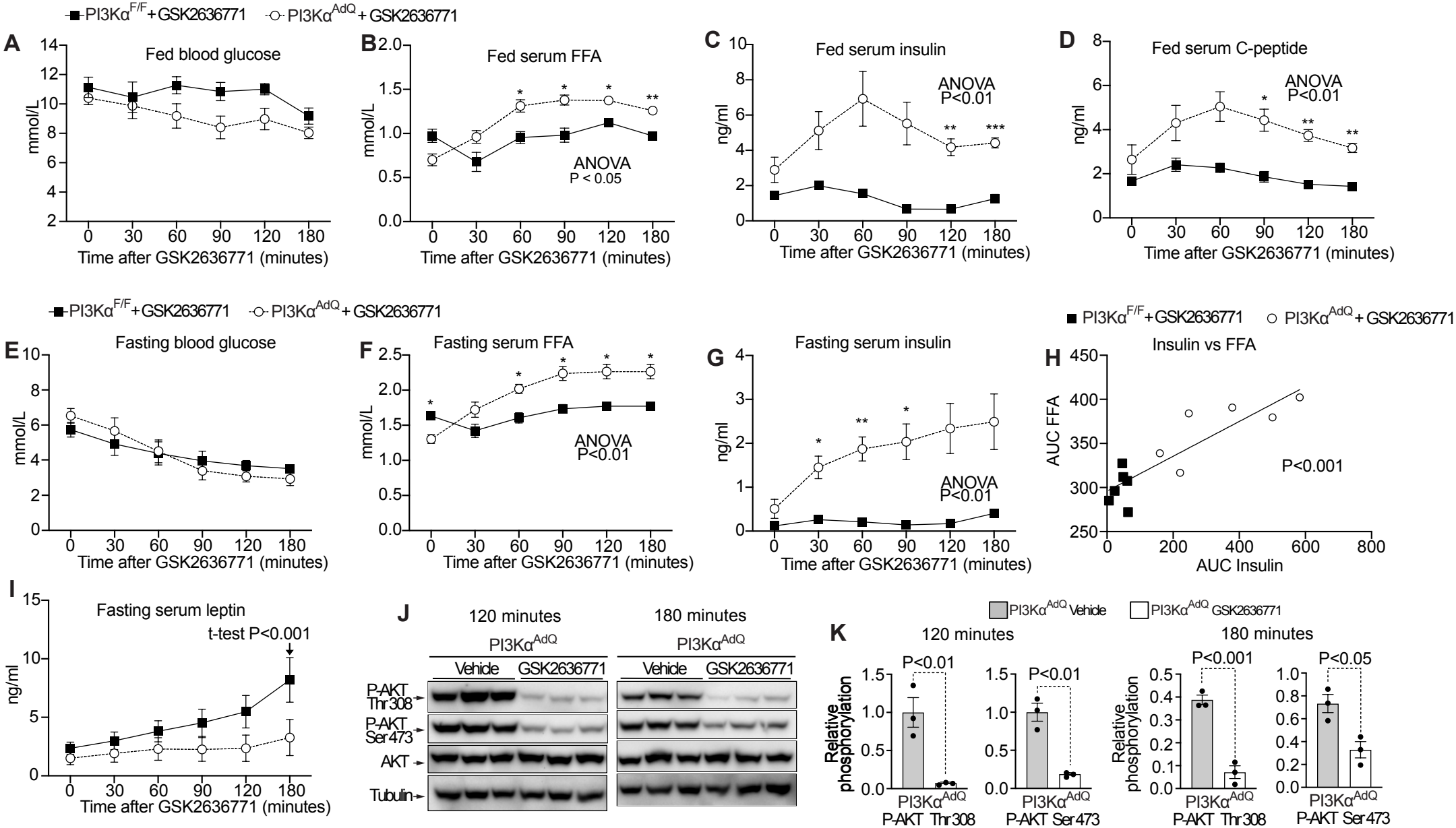
PI3Kα F/F + GSK2636771
PI3Kα AdQ + GSK2636771
A
Fed blood glucose
mmol/L
Time after GSK2636771 (minutes)
B
Fed serum FFA
mmol/L
ANOVA
P < 0.05
Time after GSK2636771 (minutes)
C
Fed serum insulin
ng/ml
ANOVA
P<0.01
Time after GSK2636771 (minutes)
D
Fed serum C-peptide
ng/ml
ANOVA
P<0.01
Time after GSK2636771 (minutes)
E
Fasting blood glucose
mmol/L
Time after GSK2636771 (minutes)
F
Fasting serum FFA
mmol/L
ANOVA
P<0.01
Time after GSK2636771 (minutes)
G
Fasting serum insulin
ng/ml
ANOVA
P<0.01
Time after GSK2636771 (minutes)
H
Insulin vs FFA
AUC FFA
AUC Insulin
P<0.001
I
Fasting serum leptin
t-test P<0.001
ng/ml
Time after GSK2636771 (minutes)
J
120 minutes
180 minutes
PI3Kα AdQ
Vehicle
GSK2636771
P-AKT Thr308
P-AKT Ser473
AKT
Tubulin
K
PI3Kα AdQ Vehicle
PI3Kα AdQ GSK2636771
120 minutes
180 minutes
Relative phosphorylation
P<0.01
P<0.01
P<0.001
P<0.05
PI3Kα AdQ
P-AKT Thr308
P-AKT Ser473

Figure 4

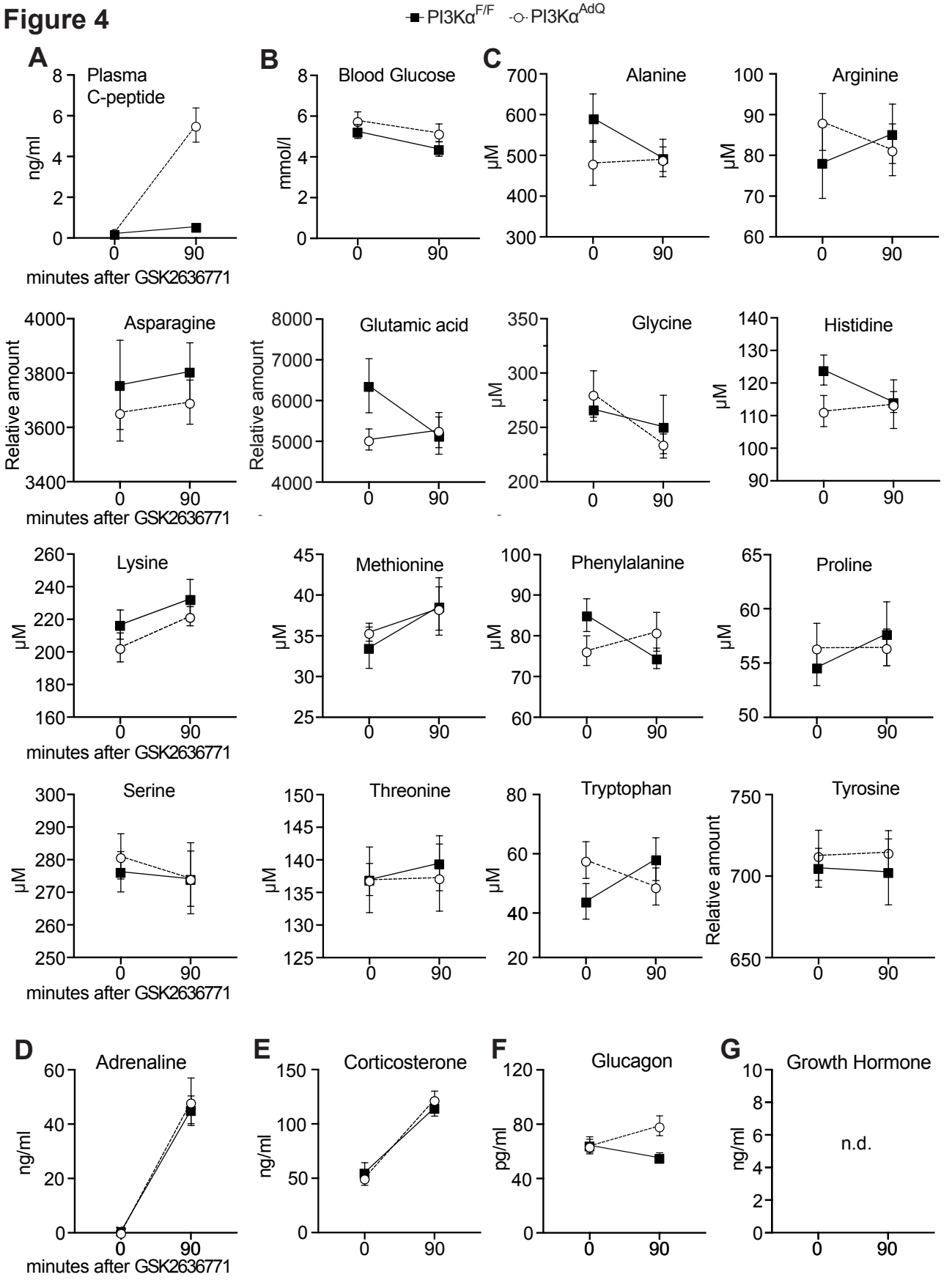
PI3Kα F/F
PI3Kα AdQ
A
Plasma C-peptide
ng/ml
minutes after GSK2636771
B
Blood Glucose
mmol/l
C
Alanine
Arginine
Asparagine
Glutamic acid
Glycine
Histidine
Lysine
Methionine
Phenylalanine
Proline
Serine
Threonine
Tryptophan
Tyrosine
Relative amount
µM
D
Adrenaline
E
Corticosterone
F
Glucagon
pg/ml
G
Growth Hormone
n.d.

Figure 5

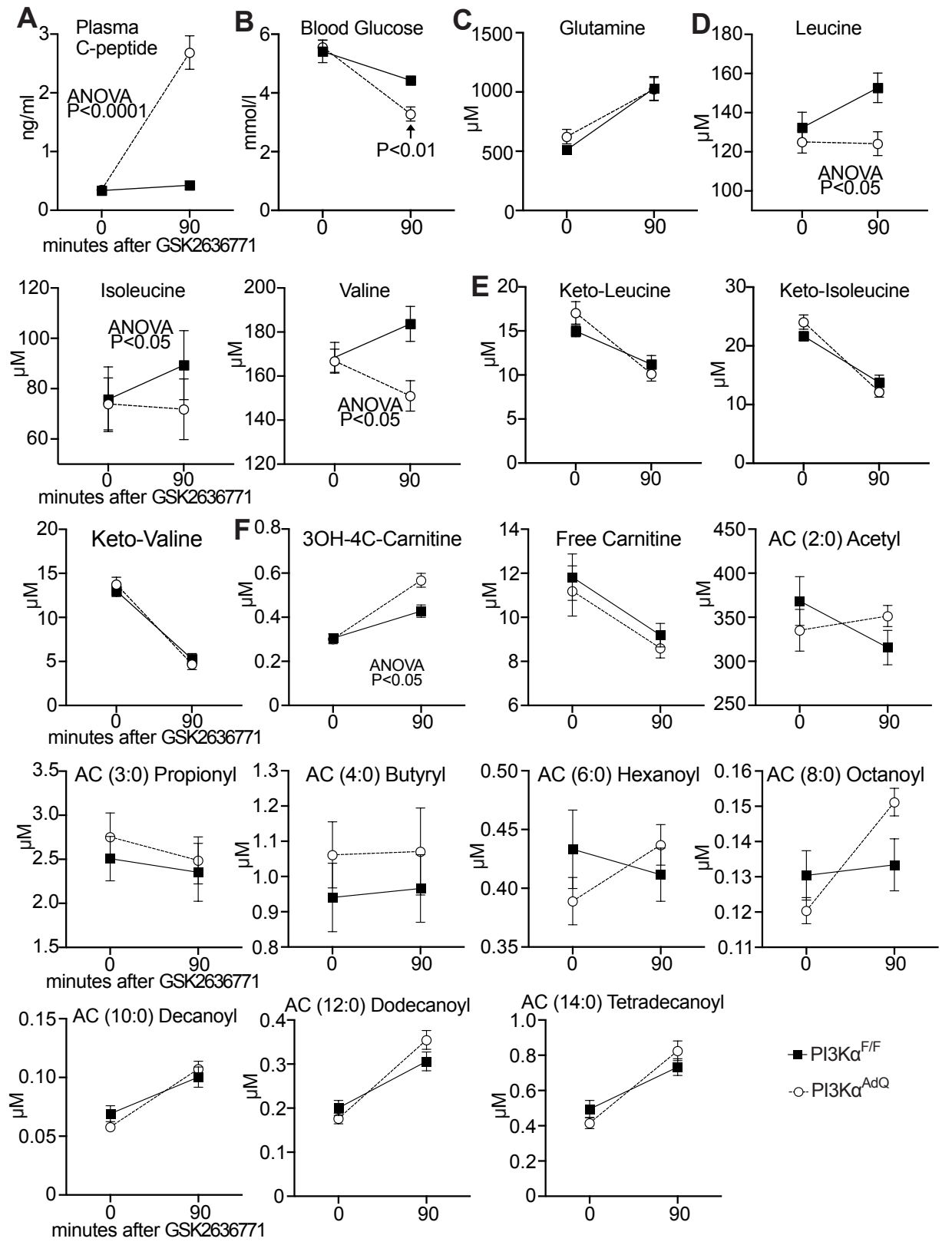
A
Plasma C-peptide
ng/ml
ANOVA P<0.0001
minutes after GSK2636771
B
Blood Glucose
mmol/l
P<0.01
C
Glutamine
μM
D
Leucine
μM
ANOVA P<0.05
Isoleucine
μM
ANOVA P<0.05
minutes after GSK2636771
Valine
μM
ANOVA P<0.05
E
Keto-Leucine
μM
Keto-Isoleucine
μM
Keto-Valine
μM
minutes after GSK2636771
F
3OH-4C-Carnitine
μM
ANOVA P<0.05
Free Carnitine
μM
AC (2:0) Acetyl
μM
AC (3:0) Propionyl
μM
minutes after GSK2636771
AC (4:0) Butyryl
μM
AC (6:0) Hexanoyl
μM
AC (8:0) Octanoyl
μM
AC (10:0) Decanoyl
μM
minutes after GSK2636771
AC (12:0) Dodecanoyl
μM
AC (14:0) Tetradecanoyl
μM
PI3Kα F/F
PI3Kα AdQ

Figure 6

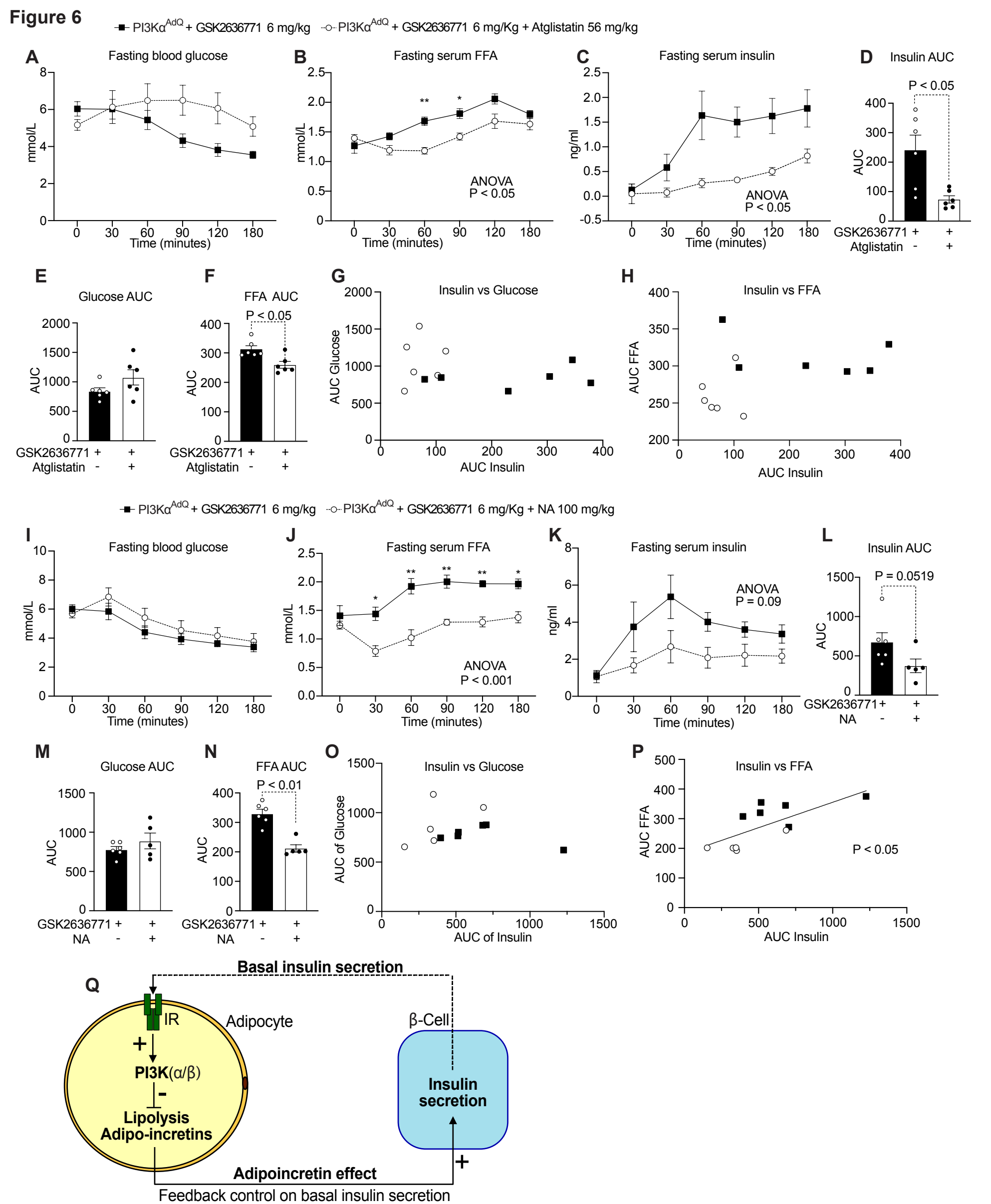
PI3Kα^AdQ + GSK2636771 6 mg/kg
PI3Kα^AdQ + GSK2636771 6 mg/Kg + Atglistatin 56 mg/kg
A
Fasting blood glucose
mmol/L
Time (minutes)
B
Fasting serum FFA
mmol/L
ANOVA
P < 0.05
Time (minutes)
C
Fasting serum insulin
ng/ml
ANOVA
P < 0.05
Time (minutes)
D
Insulin AUC
P < 0.05
AUC
GSK2636771 + +
Atglistatin - +
E
Glucose AUC
AUC
GSK2636771 + +
Atglistatin - +
F
FFA AUC
P < 0.05
AUC
GSK2636771 + +
Atglistatin - +
G
Insulin vs Glucose
AUC Glucose
AUC Insulin
H
Insulin vs FFA
AUC FFA
AUC Insulin
PI3Kα^AdQ + GSK2636771 6 mg/kg
PI3Kα^AdQ + GSK2636771 6 mg/Kg + NA 100 mg/kg
I
Fasting blood glucose
mmol/L
Time (minutes)
J
Fasting serum FFA
mmol/L
ANOVA
P < 0.001
Time (minutes)
K
Fasting serum insulin
ng/ml
ANOVA
P = 0.09
Time (minutes)
L
Insulin AUC
P = 0.0519
AUC
GSK2636771 + +
NA - +
M
Glucose AUC
AUC
GSK2636771 + +
NA - +
N
FFA AUC
P < 0.01
AUC
GSK2636771 + +
NA - +
O
Insulin vs Glucose
AUC of Glucose
AUC of Insulin
P
Insulin vs FFA
AUC FFA
P < 0.05
AUC Insulin
Q
Basal insulin secretion
IR
Adipocyte
β-Cell
+
PI3K(α/β)
-
Lipolysis
Adipo-incretins
Insulin
secretion
+
Adipoincretin effect
Feedback control on basal insulin secretion

Figure 7

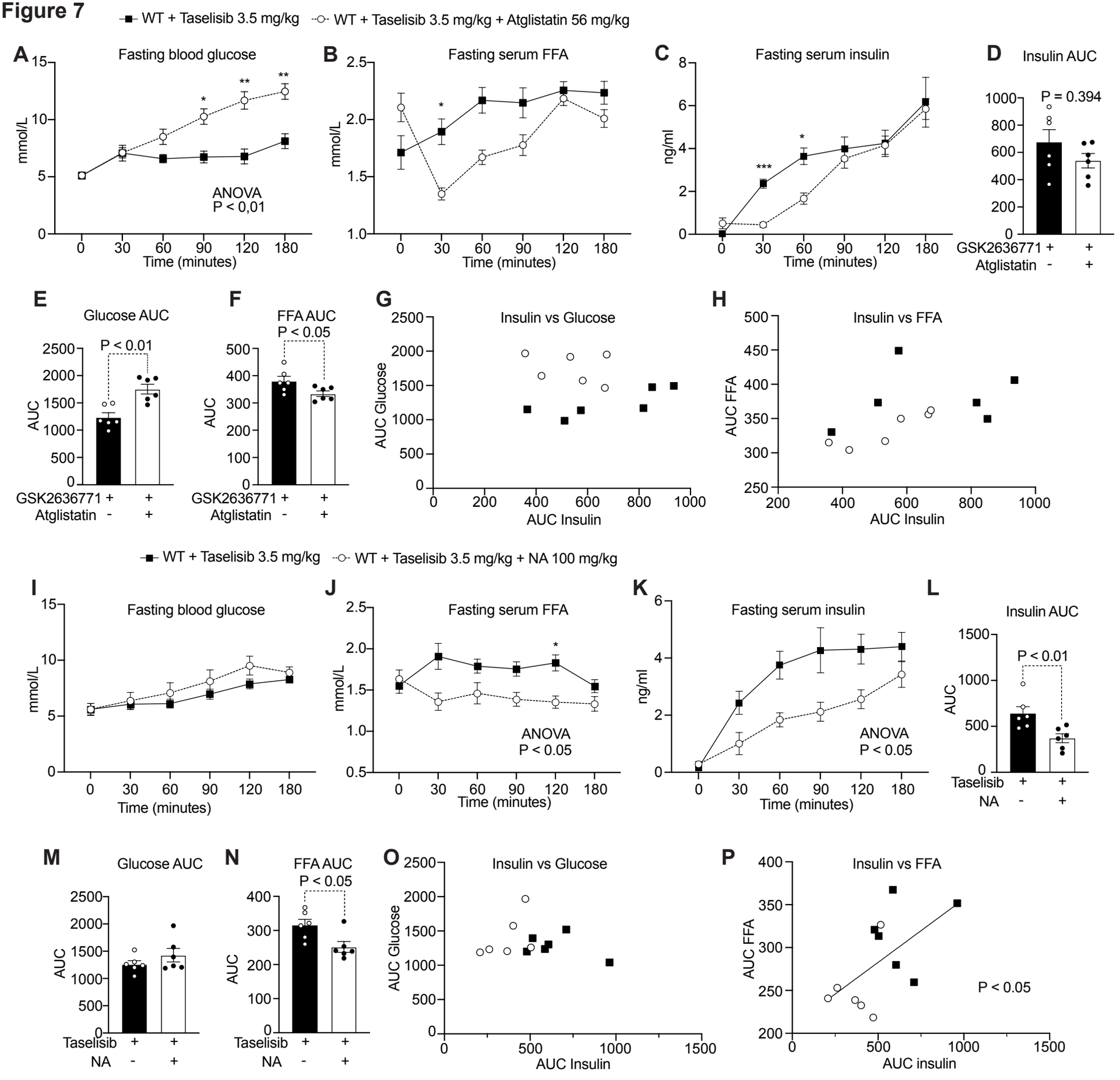
WT + Taselisib 3.5 mg/kg
WT + Taselisib 3.5 mg/kg + Atglistatin 56 mg/kg
A
Fasting blood glucose
mmol/L
ANOVA
P < 0,01
Time (minutes)
B
Fasting serum FFA
mmol/L
Time (minutes)
C
Fasting serum insulin
ng/ml
Time (minutes)
D
Insulin AUC
P = 0.394
GSK2636771
Atglistatin
E
Glucose AUC
P < 0.01
AUC
F
FFA AUC
P < 0.05
AUC
G
Insulin vs Glucose
AUC Glucose
AUC Insulin
H
Insulin vs FFA
AUC FFA
AUC Insulin
WT + Taselisib 3.5 mg/kg
WT + Taselisib 3.5 mg/kg + NA 100 mg/kg
I
Fasting blood glucose
mmol/L
Time (minutes)
J
Fasting serum FFA
mmol/L
ANOVA
P < 0.05
Time (minutes)
K
Fasting serum insulin
ng/ml
ANOVA
P < 0.05
Time (minutes)
L
Insulin AUC
P < 0.01
AUC
Taselisib
NA
M
Glucose AUC
AUC
N
FFA AUC
P < 0.05
AUC
O
Insulin vs Glucose
AUC Glucose
AUC Insulin
P
Insulin vs FFA
AUC FFA
P < 0.05
AUC insulin